Eigenvalue Based Detection of a Signal in Colored Noise: Finite and Asymptotic Analyses

Lahiru D. Chamain, *Graduate Student Member, IEEE*, Prathapasinghe Dharmawansa, *Member, IEEE*, Saman Atapattu, *Senior Member, IEEE*, and Chintha Tellambura, *Fellow, IEEE*

***Abstract*—Signal detection in colored noise with an unknown covariance matrix has a myriad of applications in diverse scientific/engineering fields. The test statistic is the largest generalized eigenvalue (l.g.e.) of the whitened sample covariance matrix, which is constructed via m-dimensional p signal-plus-noise samples and m-dimensional n noise-only samples. A finite dimensional characterization of this statistic under the alternative hypothesis has hitherto been an open problem. We answer this problem by deriving cumulative distribution function (c.d.f.) of this l.g.e. via the powerful orthogonal polynomial approach, exploiting the deformed Jacobi unitary ensemble (JUE). Two special cases and an asymptotic version of the c.d.f. are also derived. With this new c.d.f., we comprehensively analyze the receiver operating characteristics (ROC) of the detector. Importantly, when the noise-only covariance matrix is nearly rank deficient (i.e., $m = n$), we show that (a) when m and p increase such that m/p is fixed, at each fixed signal-to-noise ratio (SNR), there exists an optimal ROC profile. We also establish a tight approximation of it; and (b) asymptotically, reliable signal detection is always possible if SNR scales with m.**

***Index Terms*—Colored noise, eigenvalue, F-matrix, Hypergeometric function of two matrix arguments, Jacobi unitary ensemble, orthogonal polynomials, receiver operating characteristics (ROC), Wishart matrix**

I. Introduction

Eigenvalue based detection of a signal embedded in noise is a fundamental problem with a myriad of applications in diverse fields including signal processing, wireless communications, cognitive radio, bioinformatics and many more [1]–[9]. Thus, sample eigenvalue (of the sample covariance matrix) based detection has gained prominence recently ([10], [11] and references therein). In this context, the largest sample eigenvalue based detection, also known as Roy's largest root test [12], has been popular among detection theorists. Under the common Gaussian setting with white noise, this amounts to the use of the largest eigenvalue of a Wishart matrix having a so-called spiked covariance [13]–[18].

However, colored noise (or correlated noise) occurs in multitudes of applications [9], [19]–[23]. In this case, we can utilize the maximum eigenvalue of the matrix formed by whitening the signal-plus-noise sample covariance matrix with the noise-only sample covariance matrix. For this estimator, Nadakuditi and Silverstein [5] proposed a framework to use the generalized eigenvalues of the whitened signal-plus-noise sample covariance matrix for detection. The assumption of having the noise only sample covariance matrix is realistic in many practical situations as detailed in [5]. The fundamental *high dimensional* limits of the generalized sample eigenvalue based detection in colored noise have been thoroughly investigated in [5]. However, to our best knowledge, a tractable *finite dimensional* analysis is not available in the literature. Thus, in this paper, we characterize the statistics of Roy's largest root in the finite dimensional colored noise setting. Moreover, we investigate certain limiting behaviors of Roy's largest root to deepen our understanding of the classical detection problem in colored noise. These limiting expressions are derived based on their finite dimensional counterparts, whereas in the literature, it is customary to use entirely different tools for finite and asymptotic analyses.

The Roy's largest root of the generalized eigenvalue detection problem in the Gaussian setting amounts to finite dimensional characterization of the largest eigenvalue of the deformed Jacobi ensemble. Various asymptotic expressions (high dimensional and high signal-to-noise ratio) in this respect have been derived in [24]–[27] for the deformed Jacobi ensemble. Recently, [28], [29] have presented some finite dimensional expressions for the edges of the deformed Jacobi ensemble (i.e., maximum and minimum eigenvalues) in terms of hypergeometric functions of a single matrix argument. Since these functions do not assume simple forms in general, the resultant expressions for the edges are of little use in engineering applications. On the other hand finite dimensional expressions with different degrees of complexity are available for the Jacobi ensemble (without deformation) [30]–[33]. Although finite dimensional, some of these expressions are not amenable to further manipulations. Therefore, in this paper, we present a simple and tractable closed-form solution to the cumulative

Manuscript received February 05, 2019; revised March 26, 2020; accepted April 28, 2020. Date of publication xxx, 2020; date of current version xxx, 2020. The work of Saman Atapattu was supported in part by the Australian Research Council (ARC) through the Discovery Early Career Researcher Award (DECRA) under Grant DE160100020. This work was presented in part at the IEEE Global Communications Conference (GLOBECOM), Hawaii, USA, Dec. 2019.

L. D. Chamain is with the Department of Electrical and Computer Engineering, 2064 Kemper Hall, University of California Davis, 1 Shields Avenue, Davis, CA 95616 (e-mail: hdchamain@ucdavis.edu).

P. Dharmawansa is with the Department of Electronic and Telecommunication Engineering, University of Moratuwa, Moratuwa 10400, Sri Lanka (e-mail: prathapa@uom.lk).

S. Atapattu is with the Department of Electrical and Electronic Engineering, University of Melbourne, Parkville, VIC 3010, Australia (e-mail: saman.atapattu@unimelb.edu.au).

C. Tellambura is with the Department of Electrical and Computer Engineering, University of Alberta, Edmonton, AB T6G 2R3, Canada (e-mail: ct4@ualberta.ca).

Communicated by Prof. Radu Balan, Associate Editor for Detection and Estimation.

distribution function (c.d.f.) of the maximum eigenvalue of the deformed Jacobi ensemble. This expression further facilitates the analysis of the receiver operating characteristics (ROC) of Roy's largest root test. All these results are made possible due to a novel alternative joint eigenvalue density function that we have derived based on the contour integral approach due to [34]–[38].

The key results developed in this paper enable us to understand the joint effect of the system dimensionality (m), the number of signal-plus-noise samples (p) and noise-only samples (n), and the signal-to-noise ratio (γ) on the ROC. For instance, the relative disparity between m and n improves the ROC profile for fixed values of the other parameters. However, the general finite dimensional ROC expressions turns out to give little analytical insights. Therefore, to obtain more insights, we have particularly focused on the case for which the system dimensionality equals the number of the noise-only samples (i.e., $m = n$). Since this equality is the minimum requirement for the validity of the whitening operation, from the ROC perspective, it corresponds to the worst possible case when then other parameters being fixed. It turns out that, in this scenario, when p increases for fixed m, n and γ, the ROC profile improves. In this respect, the ROC profile converges to a limiting profile as $p \to \infty$. In contrast, when we increase p and m simultaneously such that m/p is a constant (≤ 1) for fixed γ, we can observe an optimal ROC profile for some special values of p and m. However, as $p, m, n \to \infty$ such that m/p approaches a constant (≤ 1) (the high dimensional limit) and $m/n = 1$ for fixed γ, the maximum eigenvalue tend to lose its detection power. This phenomenon amounts to stating that the maximum eigenvalue has no power below the phase transition. This has been observed in random matrix theory literature [5], [27], [39]–[41]. Be that as it may, the most interesting result emerged from our analysis is that, when γ scales with m under the latter assumptions, the ROC attains a finite limit. In other words, the maximum eigenvalue still retains its detection power in the high dimension when γ scales with m as $m \to \infty$. For instance, under Rayleigh fading, as $m \to \infty$, γ scales with m (due to the strong law of large numbers). Therefore, the above insight can be of paramount importance in designing future wireless communication systems (5G and beyond).

The remainder of this paper is organized as follows. In Section II, we formulate the classical detection problem in unknown colored noise. A new c.d.f. expression for the maximum eigenvalue (i.e., Roy's largest root) of the deformed Jacobi unitary ensemble is derived in Section III. It also gives certain particularizations of the general c.d.f. expression. Subsequently, Section IV investigates the ROC characteristics of Roy's largest root test in the light of the c.d.f. derived in Section III. Moreover, the interplay between the system dimensionality, the number of signal-plus-noise samples, and the noise-only samples has been analytically characterized in Section IV. Finally, conclusions are drawn in Section V.

Notation: The superscript $(\cdot)^\dagger$ indicates the Hermitian transpose, $\det(\cdot)$ denotes the determinant of a square matrix, $\mathrm{tr}(\cdot)$ represents the trace of a square matrix, and $\mathrm{etr}(\cdot)$ stands for $\exp(\mathrm{tr}(\cdot))$. The $n \times n$ identity matrix is represented by $\mathbf{I}_n$ and the Euclidean norm of a vector $\mathbf{w}$ is denoted by $||\mathbf{w}||$. A diagonal matrix with the diagonal entries $a_1, a_2, \ldots, a_n$ is denoted by $\mathrm{diag}(a_1, a_2, \ldots, a_n)$. We denote the $m \times m$ unitary group by $U(m)$. Finally, we use the following notation to compactly represent the determinant of an $n \times n$ block matrix:

$$\det\left[a_i \;\; b_{i,j}\right]_{\substack{i=1,2,\ldots,n \\ j=2,3,\ldots,n}} = \begin{vmatrix} a_1 & b_{1,2} & b_{1,3} & \ldots & b_{1,n} \\ a_2 & b_{2,2} & b_{2,3} & \ldots & b_{2,n} \\ \vdots & \vdots & \vdots & \ddots & \vdots \\ a_n & b_{n,2} & b_{n,3} & \ldots & b_{n,n} \end{vmatrix}.$$

II. Problem formulation

Consider the following generic signal detection problem in colored Gaussian noise

$$\mathbf{x} = \sqrt{\rho}\mathbf{h}s + \mathbf{n}$$

where $\mathbf{x}, \mathbf{h} \in \mathbb{C}^m$ are m-dimensional complex vectors, $\rho > 0$ is a signal power measure, $s \sim \mathcal{CN}(0,1)$ is a complex Gaussian transmit symbol and $\mathbf{n} \sim \mathcal{CN}_m(\mathbf{0}, \mathbf{\Sigma})$ is a random complex Gaussian noise vector with covariance matrix $\mathbf{\Sigma}$, which may or may not be known at the detector. The classical signal detection problem amounts to the following hypothesis testing problem:

$$\begin{aligned} \mathcal{H}_0 &: \ \rho = 0 \quad \text{Signal is absent} \\ \mathcal{H}_1 &: \ \rho > 0 \quad \text{Signal is present.} \end{aligned}$$

Noting that the covariance matrix of $\mathbf{x}$ can be written as

$$\mathbf{S} = \rho\mathbf{h}\mathbf{h}^\dagger + \mathbf{\Sigma},$$

the above hypothesis testing problem assumes the following equivalent form

$$\begin{aligned} \mathcal{H}_0 &: \ \mathbf{R} = \mathbf{\Sigma} \quad \text{Signal is absent} \\ \mathcal{H}_1 &: \ \mathbf{S} = \rho\mathbf{h}\mathbf{h}^\dagger + \mathbf{\Sigma} \quad \text{Signal is present.} \end{aligned}$$

If the signal-plus-noise covariance matrix $\mathbf{S}$ and the noise covariance matrix $\mathbf{\Sigma}$ were known, we may compute the matrix

$$\mathbf{\Psi} = \mathbf{R}^{-1}\mathbf{S} = \rho\mathbf{\Sigma}^{-1}\mathbf{h}\mathbf{h}^\dagger + \mathbf{I}.$$

Denote the eigenvalues of $\mathbf{\Psi}$ by $\lambda_1 \leq \lambda_2 \leq \ldots \leq \lambda_m$. These eigenvalues are in fact the generalized eigenvalues of the matrix pair $(\mathbf{S}, \mathbf{R})$. Since the rank of $\mathbf{h}\mathbf{h}^\dagger$ is one, $m-1$ eigenvalues are all equal to one ($i.e., \lambda_1 = \lambda_2 = \ldots = \lambda_{m-1} = 1$) while the remaining maximum eigenvalue of $\mathbf{\Psi}$ ($i.e., \lambda_m$) is strictly greater than one. Thus, the maximum eigenvalue of $\mathbf{\Psi}$ could be used to detect the presence of a signal [5].

In most practical settings, $\mathbf{R}$ and $\mathbf{S}$ matrices are unknown. To circumvent this difficulty, we may replace $\mathbf{R}$ and $\mathbf{S}$ by their sample estimates. To this end, we assume the availability of $p > 1$ i.i.d. signal-plus-noise samples $\{\mathbf{x}_1, \mathbf{x}_2, \ldots, \mathbf{x}_p\}$, and n i.i.d. noise-only samples $\{\mathbf{n}_1, \mathbf{n}_2, \ldots, \mathbf{n}_n\}$. Thus, the sample estimates of $\mathbf{R}$ and $\mathbf{S}$ become

$$\widehat{\mathbf{R}} = \frac{1}{n}\sum_{\ell=1}^{n} \mathbf{n}_\ell \mathbf{n}_\ell^\dagger, \tag{1}$$

$$\widehat{\mathbf{S}} = \frac{1}{p}\sum_{k=1}^{p} \mathbf{x}_k \mathbf{x}_k^\dagger \tag{2}$$

where we assume that $n, p \geq m$ (this ensures that both $\widehat{\mathbf{R}}$ and $\widehat{\mathbf{S}}$ are positive definite with probability 1 [41], [42]). Consequently, following [5], we form the matrix

$$\widehat{\mathbf{\Psi}} = \widehat{\mathbf{R}}^{-1}\widehat{\mathbf{S}} \tag{3}$$

and focus on its maximum eigenvalue as the test statistic[1]. As such, we have

$$n\widehat{\mathbf{R}} \sim \mathcal{CW}_m\left(n, \mathbf{\Sigma}\right)$$
$$p\widehat{\mathbf{S}} \sim \mathcal{CW}_m\left(p, \mathbf{\Sigma} + \rho\mathbf{h}\mathbf{h}^\dagger\right).$$

Noting that the eigenvalues of $\widehat{\mathbf{\Psi}}$ do not change under the simultaneous transformations $\widehat{\mathbf{R}} \mapsto \mathbf{\Sigma}^{-1/2}\widehat{\mathbf{R}}\mathbf{\Sigma}^{-1/2}$, and $\widehat{\mathbf{S}} \mapsto \mathbf{\Sigma}^{-1/2}\widehat{\mathbf{S}}\mathbf{\Sigma}^{-1/2}$, without loss of generality we assume that $\mathbf{\Sigma} = \sigma^2\mathbf{I}_m$. Therefore, in what follows we focus on the maximum eigenvalue of $\widehat{\mathbf{\Psi}}$, where

$$n\widehat{\mathbf{R}} \sim \mathcal{CW}_m\left(n, \mathbf{I}_m\right) \tag{4}$$
$$p\widehat{\mathbf{S}} \sim \mathcal{CW}_m\left(p, \mathbf{I}_m + \gamma\mathbf{u}\mathbf{u}^\dagger\right) \tag{5}$$

with $\gamma = \rho||\mathbf{h}||^2/\sigma^2$ and $\mathbf{u} = \mathbf{h}/||\mathbf{h}||$ being a unit vector.

Let us denote the maximum eigenvalue of $\widehat{\mathbf{\Psi}}$ as $\hat{\lambda}_{\max}(\gamma)$. Now, in order to assess the performance of the maximum-eigen based detector, we need to evaluate the detection[2] and false alarm probabilities. They may be expressed as

$$P_D(\gamma, \mu) = \Pr\left(\hat{\lambda}_{\max}(\gamma) > \mu_{\text{th}}|\mathcal{H}_1\right) \tag{6}$$

and

$$P_F(\gamma, \mu) = \Pr\left(\hat{\lambda}_{\max}(\gamma) > \mu_{\text{th}}|\mathcal{H}_0\right) \tag{7}$$

where μ_{th} is the threshold. The (P_D, P_F) pair characterizes the detector and is called the ROC profile.

Our main challenge is to characterize the maximum eigenvalue of $\widehat{\mathbf{\Psi}}$ under the alternative $\mathcal{H}_1$. This particular matrix is also referred to as the multivariate F matrix in the statistics literature [42]. It is also related to the so called Jacobi ensemble in random matrix theory [43], [44]. The joint eigenvalue distribution of the F (also Jacobi ensemble) matrix has been well documented in the literature [42], [43], [45]. The extreme eigenvalues of F under the null has been characterized in [30]–[32] in terms of hypergeometric function of one matrix argument. To gain more insights into the behavior of the extreme eigenvalues, focus has been shifted to various asymptotic domains (high dimensionality or high SNR). In this respect, various asymptotic expressions for the extreme eigenvalues, under the null, have been established in [24], [25], [46]–[50]. Recently, capitalizing on new contour integral representations of hypergeometric functions of matrix arguments by [34]–[37], [51], several new asymptotic results (including phase transition phenomena) for the maximum eigenvalue, under the alternative, have been established [26]. Also, the authors in [5], [27], [40] have employed the Stiltjes transform technique to relax the Gaussian assumption, thereby establishing the universality nature of the above results. Despite those asymptotic results, a finite-dimensional characterization of the maximum eigenvalue under the alternative hypothesis has been an open problem. Therefore, in this paper, we attack this problem by exploiting orthogonal polynomial techniques due to Mehta [43] to obtain a closed-form solution. In particular, we derive an expression which contains a determinant whose dimension depends through the relative difference between m and n. Consequently, this property is used to establish an interesting asymptotic result on the maximum eigenvalue under the alternative hypothesis.

[1]This test statistic is a consequence of Roy's union intersection principle [12].

[2]This is also known as the power of the test.

III. C.D.F. of the Maximum Eigenvalue

Before proceeding further, we present some fundamental results pertaining to the joint eigenvalue distribution of an F-matrix and Jacobi polynomials.

A. Preliminaries

Definition 1: Let $\mathbf{W}_1 \sim \mathcal{W}_m\left(p, \mathbf{\Sigma}\right)$ and $\mathbf{W}_2 \sim \mathcal{W}_m\left(n, \mathbf{I}_m\right)$ be two independent Wishart matrices with $p, n \geq m$. Then the joint eigenvalue density of the ordered eigenvalues, $\lambda_1 \leq \lambda_2 \leq \ldots \leq \lambda_m$, of $\mathbf{W}_1\mathbf{W}_2^{-1}$ is given by [45]

$$f(\lambda_1, \lambda_2, \cdots, \lambda_m) = \frac{\mathcal{K}_1(m, n, p)}{\det{}^p\left(\mathbf{\Sigma}\right)} \prod_{j=1}^{m} \lambda_j^{p-m} \Delta_m^2(\boldsymbol{\lambda}) \times {}_1\widetilde{F}_0\left(p+n; -\mathbf{\Sigma}^{-1}, \mathbf{\Lambda}\right) \tag{8}$$

where ${}_1\widetilde{F}_0\left(\cdot;\cdot,\cdot\right)$ is the generalized complex hypergeometric function of two matrix arguments, $\Delta_m(\boldsymbol{\lambda}) = \prod_{1\leq i<j\leq m}\left(\lambda_j - \lambda_i\right)$ is the Vandermonde determinant, $\mathbf{\Lambda} = \text{diag}\left(\lambda_m, \ldots, \lambda_1\right)$, and

$$\mathcal{K}_1(m, n, p) = \frac{\pi^{m(m-1)}\widetilde{\Gamma}_m(n+p)}{\widetilde{\Gamma}_m(m)\widetilde{\Gamma}_m(n)\widetilde{\Gamma}_m(p)}$$

with the complex multivariate gamma function is written in terms of the classical gamma function $\Gamma(\cdot)$ as

$$\widetilde{\Gamma}_m(n) = \pi^{\frac{1}{2}m(m-1)} \prod_{j=1}^{m} \Gamma\left(n-j+1\right).$$

Definition 2: Jacobi polynomials can be defined, for $a, b > -1$, as follows [52, eq. 5.112]

$$P_n^{(a,b)}(x) = \sum_{k=0}^{n} \binom{n+a}{n-k}\binom{n+k+a+b}{k}\left(\frac{x-1}{2}\right)^k \tag{9}$$

where $\binom{n}{k} = \frac{n!}{(n-k)!k!}$ with $n \geq k \geq 0$.
We may alternatively express the Jacobi polynomial as [52]

$$P_n^{(a,b)}(x) = \binom{n+a}{a} {}_2F_1\left(-n, n+a+b+1; 1+a; \frac{1-x}{2}\right) \tag{10}$$

where ${}_2F_1(\cdot;\cdot;\cdot)$ is the Gauss hypergeometric function. Following (10), the successive derivatives of the Jacobi polynomial can be written as

$$\frac{\mathrm{d}^k}{\mathrm{d}x^k} P_n^{(a,b)}(x) = 2^{-k}(n+a+b+1)_k P_{n-k}^{(a+k,b+k)}(x) \tag{11}$$

where $(a)_k = a(a+1)\dots(a+k-1)$ with $(a)_0 = 1$ denotes the Pochhammer symbol. It is noteworthy that, for a negative integer $-n$ with $n \in \mathbb{Z}^+$, we have [52]

$$(-n)_k = \begin{cases} \frac{(-1)^k n!}{(n-k)!} & \text{if } 0 \le k \le n \\ 0 & \text{if } k > n. \end{cases}$$

B. Finite Dimensional Analysis of the C.D.F.

Armed with these preliminary definitions, now we focus on deriving the new c.d.f. for the maximum eigenvalue of $\mathbf{W}_1\mathbf{W}_2^{-1}$ when the covaraince matrix $\mathbf{\Sigma}$ takes the so called rank-1 spiked form. That is, the covariance matrix can be decomposed as

$$\mathbf{\Sigma} = \mathbf{I}_m + \eta\mathbf{v}\mathbf{v}^\dagger = \mathbf{V}\text{diag}\left(1+\eta, 1, 1, \dots, 1\right)\mathbf{V}^\dagger \tag{12}$$

where $\mathbf{V} = (\mathbf{v}\ \mathbf{v}_2\ \dots \mathbf{v}_m) \in \mathbb{C}^{m\times m}$ is a unitary matrix and $\eta \ge 0$. Before developing our method, it is important to highlight the difficulty of a direct solution via (8). Following Khatri [53], the hypergeometric function of two matrix arguments given in the join density (8) can be written as a ratio between the determinants of two $m \times m$ square matrices. Since the eigenvalues of the matrix $\mathbf{\Sigma}^{-1}$ are such that $1/(1+\eta)$ has algebraic multiplicity one and 1 has algebraic multiplicity $m-1$, the resultant ratio takes an indeterminate form. Therefore, one has to repeatedly apply L'Hospital's rule to obtain a deterministic expression. However, the resulting expression is not amenable to apply Mehta's [43] orthogonal polynomial technique. Therefore, to apply it, we first derive an alternative joint eigenvalue density expression. This alternative derivation technique has also been used earlier in [34] to derive a single contour integral representation for the joint eigenvalue density when the matrices are real[3]. The following corollary gives the alternative joint density expression.

Corollary 3: Let $\mathbf{W}_1 \sim \mathcal{W}_m(p, \mathbf{I}_m + \eta\mathbf{v}\mathbf{v}^\dagger)$ and $\mathbf{W}_2 \sim \mathcal{W}_m(n, \mathbf{I}_m)$ be independent Wishart matrices with $m \le p, n$ and $\eta \ge 0$. Then the joint density of the ordered eigenvalues $0 \le \lambda_1 \le \lambda_2 \le \dots \le \lambda_m < \infty$ of $\mathbf{W}_1\mathbf{W}_2^{-1}$ is given by

$$f(\lambda_1, \lambda_2, \dots, \lambda_m) = f_{\text{uc}}(\lambda_1, \lambda_2, \dots, \lambda_m) f_{\text{cor}}(\lambda_1, \lambda_2, \dots, \lambda_m) \tag{13}$$

where

$$f_{\text{uc}}(\lambda_1, \lambda_2, \dots, \lambda_m) = \mathcal{K}_1(m,n,p) \prod_{j=1}^{m} \frac{\lambda_j^{p-m}}{(1+\lambda_j)^{p+n}} \Delta_m^2(\boldsymbol{\lambda}), \tag{14}$$

$$\begin{aligned} &f_{\text{cor}}(\lambda_1, \lambda_2, \dots, \lambda_m) \\ &\quad = \frac{\mathcal{K}_2(m,n,p)}{\eta^{m-1}(1+\eta)^{p+1-m}} \prod_{j=1}^{m}(1+\lambda_j) \\ &\qquad \times \sum_{k=1}^{m} \frac{(1+\lambda_k)^{p+n-1}}{\prod_{\substack{j=1 \\ j\ne k}}^{m}(\lambda_k - \lambda_j)\left(1 + \frac{\lambda_k}{\eta+1}\right)^{p+n+1-m}}, \end{aligned}$$

and

$$\mathcal{K}_2(m,n,p) = \frac{(m-1)!\,(p+n-m)!}{(p+n-1)!}.$$

Proof: See Appendix A.

Remark 4: It is worth noting that the function $f_{\text{uc}}(\lambda_1, \lambda_2, \cdots, \lambda_m)$ denotes the joint density of the ordered eigenvalues of $\mathbf{W}_1\mathbf{W}_2^{-1}$ corresponding to the case $\mathbf{W}_1 \sim \mathcal{W}_m(p, \mathbf{I}_m)$ and $\mathbf{W}_2 \sim \mathcal{W}_m(n, \mathbf{I}_m)$.

To facilitates further analysis, noting that the continuous mapping $h : x \mapsto \frac{x}{x+1},\ x \ge 0$ is strictly increasing (i.e., order preserving), we use the variable transformations

$$x_j = \frac{\lambda_j}{1+\lambda_j},\ \ j = 1, 2, \cdots, m, \tag{15}$$

with the associated Jacobian $\left|\frac{\partial(x_1, x_2, \dots, x_m)}{\partial(\lambda_1, \lambda_2, \dots, \lambda_m)}\right| = \prod_{j=1}^{m}(1-x_j)^2$, in (13) to obtain the joint density of $0 \le x_1 \le x_2 \le \cdots \le x_m < 1$ as

$$\begin{aligned} &g(x_1, x_2, \dots, x_m) \\ &\quad = \frac{f\left(\frac{x_1}{1-x_1}, \frac{x_2}{1-x_2}, \dots, \frac{x_m}{1-x_m}\right)}{\left|\frac{\partial(x_1, x_2, \dots, x_m)}{\partial(\lambda_1, \lambda_2, \dots, \lambda_m)}\right|} \\ &\quad = \frac{\mathcal{K}_3(m,n,p)}{\eta^{m-1}(1+\eta)^{p+1-m}} \Delta_m^2(\mathbf{x}) \prod_{j=1}^{m} x_j^{p-m}(1-x_j)^{n-m} \\ &\qquad \times \sum_{k=1}^{m} \frac{1}{\prod_{\substack{j=1 \\ j\ne k}}^{m}(x_k - x_j)\left(1 - \frac{\eta}{\eta+1}x_k\right)^{p+n+1-m}} \end{aligned} \tag{16}$$

where $\mathcal{K}_3(m,n,p) = \mathcal{K}_1(m,n,p)\mathcal{K}_2(m,n,p)$.

The joint eigenvalue density (16) in turn facilitates the use of Mehta's orthogonal polynomial approach in our subsequent c.d.f. analysis.

Remark 5: Alternatively, (16) represents the joint density of the ordered eigenvalues of *deformed Jacobi ensemble*, $\mathbf{W}_1(\mathbf{W}_2 + \mathbf{W}_1)^{-1}$ with $\mathbf{W}_1 \sim \mathcal{W}_m(p, \mathbf{I}_m + \eta\mathbf{v}\mathbf{v}^\dagger)$ and $\mathbf{W}_2 \sim \mathcal{W}_m(n, \mathbf{I}_m)$.

We now consider the main contribution of this paper, namely, the derivation of the c.d.f. of the maximum eigenvalue. By the definition, the c.d.f. of $x_{\max}$ (i.e., x_m) can be written as,

$$\begin{aligned} F_{x_{\max}}(t) &= \Pr(x_{\max} \le t) \\ &= \int_{0 \le x_1 \le x_2 \le \cdots \le x_m \le t} g(x_1, x_2, \dots, x_m)\mathrm{d}\mathbf{x} \end{aligned} \tag{17}$$

where, for notational concision, we have used $\mathrm{d}\mathbf{x} = \mathrm{d}x_1\mathrm{d}x_2\dots\mathrm{d}x_m$. By evaluating the above Selberg-type integral, the c.d.f. of $x_{\max}$ can be found and hence the c.d.f. of $\lambda_{\max}$, which is given by the the following theorem.

Theorem 6: Let $\mathbf{W}_1 \sim \mathcal{W}_m(p, \mathbf{I}_m + \eta\mathbf{v}\mathbf{v}^\dagger)$ and $\mathbf{W}_2 \sim \mathcal{W}_m(n, \mathbf{I}_m)$ be independent with $m \le p, n$ and $\eta \ge 0$. Then the c.d.f. of the maximum eigenvalue $\lambda_{\max}$ of $\mathbf{W}_1\mathbf{W}_2^{-1}$ is given by

$$\begin{aligned} F_{\lambda_{\max}}^{(\alpha)}(t;\eta) &= \frac{\mathcal{K}(m,p,\alpha)}{(p-1)!\,(1+\eta)^p}\left(\frac{t}{1+t}\right)^{m(\alpha+\beta+m)} \\ &\quad \times \det\left[\Phi_i(t,\eta) \quad \Psi_{i,j}(t)\right]_{\substack{i=1,2,\dots,\alpha+1 \\ j=2,3,\dots,\alpha+1}} \end{aligned} \tag{18}$$

[3]However, when the matrices are real, the hypergeometric function of two matrix arguments does not admit such a determinant representation.

where

$$\Psi_{i,j}(t) = (m+i+\beta-1)_{j-2} P_{m+i-j}^{(j-2,\beta+j-2)}\left(\frac{2}{t}+1\right),$$

$$\Phi_i(t,\eta) = \mathcal{Q}_i(m,n,p)\sum_{k=0}^{\alpha-i+1}\frac{(p+i-1)_k(\alpha-i+2)!}{k!\,(p+m+2i-2)_k(\alpha-i-k+1)!} \times \frac{(\eta t)^{k+i-1}\left((1+\eta)(1+t)\right)^{p+k}}{(1+\eta+t)^{p+k+i-1}},$$

$$\mathcal{Q}_i(m,n,p) = \frac{(n+p+i-2)!\,(p+i-2)!}{(p+m+2i-3)!},$$

and

$$\mathcal{K}(m,p,\alpha) = \prod_{j=0}^{\alpha-1}\frac{(p+m+j-1)!}{(p+m+2j)!}$$

with $\alpha = n-m$ and $\beta = p-m$.

Proof: See Appendix B.

Remark 7: Alternatively, $\Phi_{\rm i}(t,\eta)$ can be expressed in terms of Gauss hypergeometric function as follows

$$\Phi_i(t,\eta) = \mathcal{Q}_i(m,n,p)\left(\frac{\eta t}{(1+\eta)(1+t)}\right)^{i-1} \times {}_2F_1\left(\beta+m+i-1, n+p+i-1; \beta+2m+2i-2; \frac{\eta t}{(1+\eta)(1+t)}\right). \tag{19}$$

The new exact c.d.f. expression for the maximum eigenvalue of $\mathbf{W}_1\mathbf{W}_2^{-1}$, which contains the determinant of a square matrix whose dimension depends on the difference $\alpha = n-m$, is highly desirable when the difference between m and n is small irrespective of their individual magnitudes. For instance, when $n = m$ (i.e., $\alpha = 0$) the determinant vanishes and we obtain a scalar result. This concise result is one of the many advantages of using the orthogonal polynomial approach. This key representation also facilitates the derivation of the limiting distribution of the maximum eigenvalue (when $m, n \to \infty$ such that $m-n$ is fixed).

For some special values of α and η, the c.d.f. expression (18) admits the following simple forms.

Corollary 8: The exact c.d.f. of the maximum eigenvalue of $\mathbf{W}_1\mathbf{W}_2^{-1}$ when $\eta = 0$ is given by

$$F_{\lambda_{\max}}^{(\alpha)}(t;0) = \mathcal{K}(m,p,\alpha)\frac{(n+p-1)!}{(m+p-1)!}\left(\frac{t}{1+t}\right)^{m(\alpha+\beta+m)} \times \det\left[\Psi_{i+1,j+1}(t)\right]_{i,j=1,2,\ldots,\alpha}. \tag{20}$$

Proof: Following (19), it is easy to see that, when $\eta = 0$, all the elements in the first column of the determinant in (18) become zero except the first entry which is $(p-1)!\,(n+p-1)!\,/(m+p-1)!$. Therefore, we expand the determinant with its first column and shift the indices i and j to conclude the proof.

Alternative expressions for c.d.f and p.d.f. of $x_{\max}$ ($x_{\max} = \lambda_{\max}/(1+\lambda_{\max})$) in the same scenario ($\eta = 0$) are given in [30] and [31], respectively. However, these results are fundamentally structurally different from our expression (20), since they contain complex hypergeometric functions of one matrix argument. In particular, the matrix argument in [30] assumes the form $t\mathbf{I}_m$, whereas the matrix argument in [31] takes the form $t\mathbf{I}_{\alpha-1}$. Further simplification of these expressions requires the repeated application of L'Hospital's rule followed by the evaluation of the resultant determinants, a cumbersome process. In contrast, the c.d.f. expression (20) does not suffer from these drawbacks.

Corollary 9: The exact c.d.f. of the maximum eigenvalue of $\mathbf{W}_1\mathbf{W}_2^{-1}$ when $\alpha = 0$ is given by ($t \geq 0$)

$$F_{\lambda_{\max}}^{(0)}(t;\eta) = \frac{\left(\frac{t}{1+t}\right)^{mp}}{\left(1+\frac{\eta}{1+t}\right)^{p}}. \tag{21}$$

Proof: When $\alpha = 0$, the determinant in (18) reduces to a single term given by

$$\Phi_1(t,\eta) = (p-1)!\,{}_2F_1\left(p, n+p; n+p; \frac{\eta t}{(1+\eta)(1+t)}\right).$$

Noting that ${}_2F_1(a,b;b;z) = {}_1F_0(a;z) = (1-z)^{-a}$ with some algebraic manipulations concludes the proof.

In the sequel, this remarkably simple result (21) is used to establish an important high dimensional limit for the maximum eigenvalue. Also, we have, for $\eta_2 > \eta_1 > 0$,

$$F^{(0)}(t;\eta_2) < F^{(0)}(t;\eta_1) < F^{(0)}(t;0).$$

Having established the finite dimensional c.d.f. results, we now focus on the asymptotic characterization of the maximum eigenvalue.

C. Asymptotic Analysis of the C.D.F.

Here we characterize the asymptotic behavior of the maximum eigenvalue of $\mathbf{W}_1\mathbf{W}_2^{-1}$ by deriving various limiting c.d.f. expressions for (18). In particular, we focus on suitably centered and scaled maximum eigenvalue in the following two important scenarios:

1) As $m, n, p \to \infty$ such that α, β, and η are fixed,
2) As $m, n, p, \eta \to \infty$ such that $\frac{m}{n} \to 1$, $\frac{m}{p} \to c \in (0,1]$, and $\frac{\eta}{m} \to \theta \geq 0$.

Asymptotic behavior of the Jacobi ensemble has been thoroughly studied in the literature (see [44], [46], [47], [48]–[50] and references therein). For instance, Johnstone [46] has shown that, for a large class of Jacobi ensembles, properly centered and scaled maximum eigenvalue (the high dimensional limit) admits a Tracy-Widom type limiting distribution. Recently, Ioana [31] has derived a new limiting p.d.f. expression for the maximum and minimum eigenvalues of the Jacobi ensemble for certain new asymptotic regimes. Despite the differences in the asymptotic regimes of their choice, one common features of all the above mentioned investigations is that $\mathbf{W}_1$ and $\mathbf{W}_2$ are white Wishart matrices. In contrast, more recently, high dimensional limit of the maximum eigenvalue

(including the so called universality) has been established when $\mathbf{W}_2$ has certain spiked covariance structures (akin to the structure given in (12)) [5], [26], [27] [39], [40]. Most importantly those authors have observed a so called phase transition (also known as BBP phase transition) phenomena associated with the maximum eigenvalue. In a nutshell, phase transition means, in the high dimensional limit, when η is below a certain critical threshold, the maximum eigenvalue does not separate from the rest of the eigenvalues[4], whereas when η is above the threshold, it separates from the rest of the eigenvalues[5]. Despite all these efforts, the behavior of the maximum eigenvalue in the above two asymptotic regimes have not been addressed in the literature. Therefore, in what follows we give limiting c.d.f. expressions pertaining to the above two scenarios.

Theorem 10: As m, p and n tend to ∞ such that $\alpha = m-n$, $\beta = p-m$, and η are fixed, the centered and scaled maximum eigenvalue $(1+\lambda_{\max})/m^2$ converges in distribution to a random variable X with the c.d.f. $F_X^{(\alpha)}(x)$. In particular, we have

$$\lim_{m\to\infty} F^{(\alpha)}_{\frac{1+\lambda_{\max}}{m^2}}(x) = F_X^{(\alpha)}(x) = \exp\left(-\frac{1}{x}\right)\det\left[\mathcal{I}_{j-i}\left(\frac{2}{\sqrt{x}}\right)\right]_{i,j=1,\cdots,\alpha} \tag{22}$$

where $\mathcal{I}_k(z)$ is the k-th order modified Bessel function of the first kind.

Proof: See Appendix D.

It is interesting to see that the limiting c.d.f. is independent of η. Due to this independence, (22) should be the limiting c.d.f. for $\eta = 0$ as well. However, an alternative expression for the limiting p.d.f. of $x_{\max}$ when $\eta = 0$ has been given in [31]. That particular expression contains a hypergeometric function of one matrix argument, and therefore does not admit a simple form. In contrast, the limiting c.d.f. (22) is simple from the representation as well as numerical evaluation perspectives. Since (22) has the same form under both hypotheses, the maximum eigenvalue based test does not have power in this particular regime.

The following theorem characterizes the maximum eigenvalue in one of the most important high dimensional settings outlined in the above second scenario.

Theorem 11: As m, p, n, and η tend to ∞ such that $m/n \to 1$, $m/p \to c \in (0,1]$, and $\eta/m \to \theta \geq 0$, the centered and scaled maximum eigenvalue $(1+\lambda_{\max})/m^2$ converges in distribution to a random variable X with the c.d.f. $F_X^{(0)}(x;c,\theta)$. In particular, we have

$$\lim_{m\to\infty} F^{(0)}_{\frac{1+\lambda_{\max}}{m^2}}(x;\theta m) = F_X^{(0)}(x;c,\theta) = \exp\left(-\frac{1+\theta}{cx}\right).$$

[4]To be precise, it converges almost surely to the upper support of the limiting spectral density [5], [26], [40].

[5]It converges almost surely to a location above the upper support of the limiting spectral density [5], [26], [40].

Proof: Following (21), we take $\alpha = 0$ and $p = m/c$ to yield

$$F^{(0)}_{\lambda_{\max}}(x;\eta) = \frac{\left(\frac{x}{1+x}\right)^{m^2/c}}{\left(1+\frac{\eta}{1+x}\right)^{m/c}},$$

from which we obtain, noting that $\eta = \theta m$,

$$\lim_{m\to\infty} F^{(0)}_{\frac{1+\lambda_{\max}}{m^2}}(x;\theta m) = F_X^{(0)}(x;c,\theta) = \lim_{m\to\infty}\frac{\left(1-\frac{1}{xm^2}\right)^{m^2/c}}{\left(1+\frac{\theta}{xm}\right)^{m/c}}. \tag{23}$$

The final result now follows by evaluating the limits as $m \to \infty$.

This remarkably simple limiting c.d.f. sheds some new light on the behavior of the maximum eigenvalue in this particular asymptotic domain. Following [5], [54], we can easily show that, for $m/n \to 1$ and $m/p \to c \in (0,1]$, the upper support of the limiting spectral density diverges to infinity[6] for fixed η. Therefore, under this scaling, the operational regime is below the phase transition, where the maximum eigenvalue has *no detection power* [5], [26]. In contrast, when η also scales with m, it turns out that (see next section), the maximum eigenvalue *has detection power* as shown in Theorem 11. The reason is that all the earlier results treated η as a constant when dealing with the high dimensional limits. This new simple result shows that, when n, p and η scale with m, an interesting new phenomenon occurs.

The above facts are clearly depicted in Figs. 1, 2 and 3 where we have used $c = 0.4$ and $m = 200$ for simulation purposes. In particular, Fig. 1 compares simulation and theoretical results for no signal case (i.e., $\eta = 0$) with a weak signal case (i.e., $\eta = 5 << m$). As can be seen from the graphs, in the high dimensional setting, the centered and scaled $\lambda_{\max}$ has the same limiting distribution (i.e., $f_X(x) = \exp(-1/cx)/cx^2$) under the both settings. This stems form the fact that the above both settings result in $\theta = 0$. In contrast, as can be seen from Figs. 2 and 3, the centered and scaled $\lambda_{\max}$ can be used to detect a strong signal in the high dimensional setting. Figure 2 compares the simulation results with the analytical limiting p.d.f. expression based on Theorem 11 for different θ values. Clearly, the strong signal bearing case can easily be identified from the no signal case in the asymptotic domain. The behavior of the limiting p.d.f. for various values of θ is depicted in Fig. 3. The dependency of the peak of the p.d.f. (i.e., $4ce^{-2}/(1+\theta)$) on θ is clearly visible from the figure.

Having armed with the finite and asymptotic characteristics of the maximum eigenvalue of $\mathbf{W}_1\mathbf{W}_2^{-1}$, we next focus on the ROC curve of the maximum eigenvalue based detector.

IV. ROC of the Maximum Eigenvalue of $\widehat{\mathbf{\Psi}}$

We now investigate the behavior of detection and false alarm probabilities of the maximum eigenvalue based test. To

[6]Following [54], [55] we can show that the exact limiting spectral density takes the form $\frac{\sqrt{x-a}}{\pi x(x+c)}$, where $a = (1-c)^2/4 \leq x < \infty$.

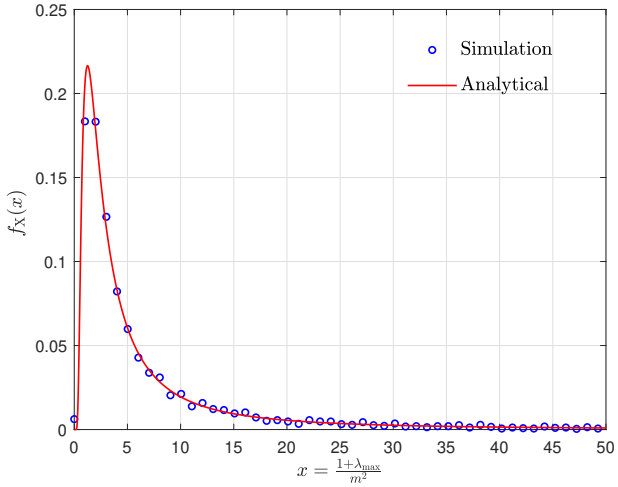

(a) $\eta = 0$ (i.e., no signal case)

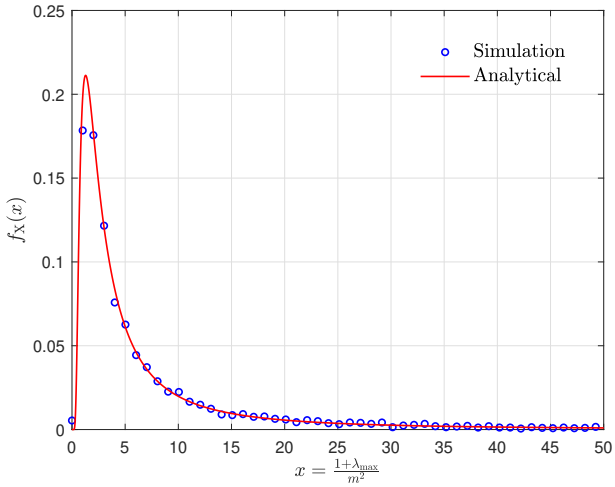

(b) $\eta = 5$ (i.e., weak signal case)

Fig. 1: Comparison of simulation and theoretical limiting p.d.f. expressions in the no signal case and weak signal case. The results are shown for $m = 200$ and $c = 0.4$.

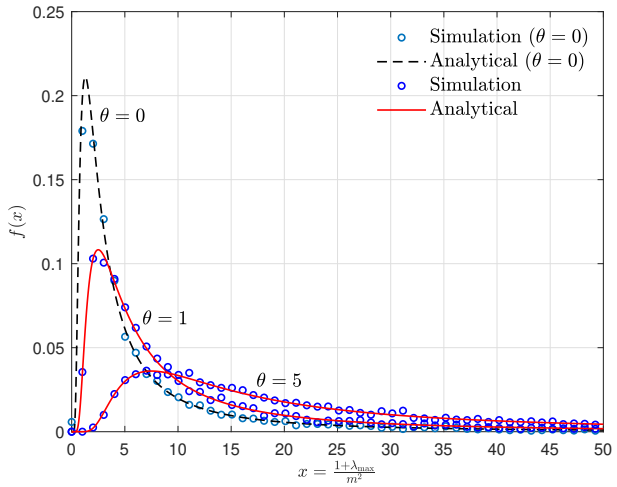

Fig. 2: Comparison of the theoretical and simulation p.d.f.s of the centered and scaled $\lambda_{\max}$ for $m/n \to 1$, $m/p \to 0.4$, and various values of $\eta/m \to \theta$ with $m = 200$.

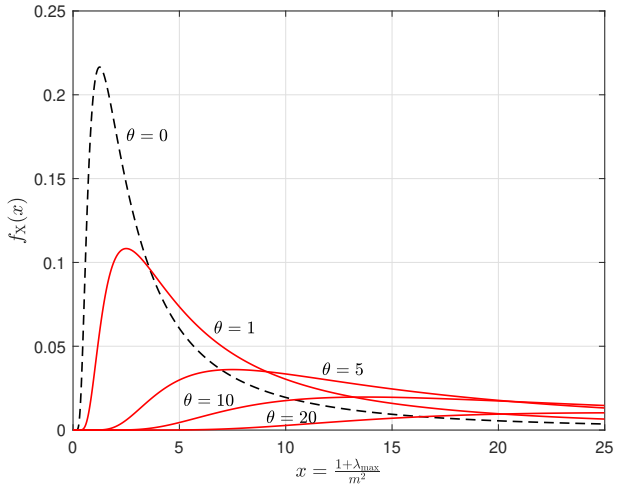

Fig. 3: Behavior of the centered and scaled $\lambda_{\max}$ for $m/n \to 1$, $m/p \to 0.4$, and various values of $\eta/m \to \theta$ with $m = 200$.

this end, noting that the eigenvalues of $\widehat{\mathbf{\Phi}}$ and $\mathbf{W}_1\mathbf{W}_2^{-1}$ are related by $\hat{\lambda}_j = (n/p)\lambda_j$, for $j = 1, 2, \ldots, m$, we represent the c.d.f. of the maximum eigenvalue corresponding to $\widehat{\mathbf{\Phi}}$ as $F^{(\alpha)}_{\lambda_{\max}}(\kappa x; \gamma)$, where $\kappa = p/n$. For convenient presentation, we treat the finite dimensional and asymptotic behaviors of the ROC in two separate sub sections.

A. Finite Dimensional Analysis

We first consider the case where matrix dimensions $(m, n,$ and $p)$ are finite. Now following Theorem 6 and Corollary 8 along with with (6), (7), the detection and false alarm probabilities can be written, respectively, as

$$P_D(\gamma, \mu_{\text{th}}) = 1 - F^{(\alpha)}_{\lambda_{\max}}(\kappa\mu_{\text{th}}; \gamma) \tag{24}$$

$$P_F(\mu_{\text{th}}) = 1 - F^{(\alpha)}_{\lambda_{\max}}(\kappa\mu_{\text{th}}; 0). \tag{25}$$

In general, deriving a functional relationship between P_D and P_F by eliminating the parametric dependency on μ_{th} is challenging. However, when α admits zero, an explicit relationship between them is specified in Corollary 12.

Corollary 12: For notational brevity, we suppress the parameters γ and μ_{th} and represent the detection and false alarm probabilities, simply as P_D and P_F. Then, when $\alpha = 0$, P_D and P_F are functionally related as

$$P_D = 1 - \frac{1 - P_F}{\left(1 + \gamma - \gamma\left[1 - P_F\right]^{1/mp}\right)^p}. \tag{26}$$

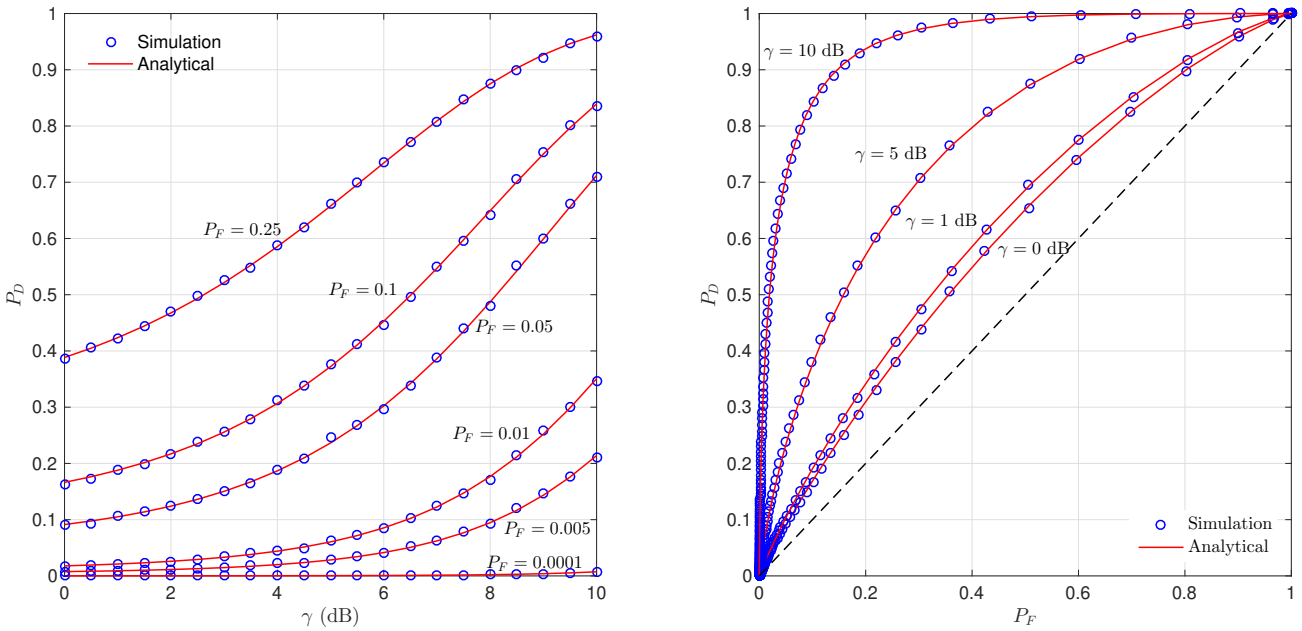

(a) P_D vs γ for different values of P_F.

(b) P_D vs P_F for different valued of γ.

Fig. 4: Probability of detection, P_D, as a function of γ and P_F for $(m, n, p) = (5, 8, 10)$.

From (26), having considered P_D as a function of γ, we can easily see that, for $\gamma_1 > \gamma_2$ and fixed m, p, and n,

$$P_D(\gamma_2) > P_D(\gamma_1).$$

This confirms the common observation that the SNR is positively correlated with the detection probability for a fixed value of P_F.

The ROC curves corresponding to different parameter settings are shown in Figs. 4 and 5. Figure 4a depicts the power profile as a function of SNR for different P_F values. As can be seen, for a fixed P_F, the power increase with the SNR, which is consistent with our intuition. The ROC of the maximum eigenvalue based detector is shown in Fig. 4b for several SNR (γ) values, which clearly shows that ROC profile improves with the increasing SNR. Since the next important parameter determining the ROC profile is the dimensionality of the covariance matrices, we investigate its effect on the ROC profile. To this end, Fig. 5a shows the effect of m/n for $m/p = 1$. As can be seen, the disparity between m and n improves the ROC profile. The reason behind this observation is that the quality of the sample covariance matrix is improved when the length of the data record (n) increases in comparison with the dimensionality of the receiver (m). Since the minimum requirement for $\widehat{\mathbf{R}}$ to be invertible is $m = n$, we can observe the worst ROC performance corresponds to $m/n = 1$. Therefore, the effect of m/p on the ROC for $m/n = 1$ is shown in Fig. 5b. As can be seen, for constant p, increasing m degrades the ROC profile. Since we have a closed-form ROC equation for $m/n = 1$, we conduct a deeper investigation on the joint effect of m and p on the ROC.

The joint effect of m and p is characterized in two scenarios. In particular, we consider i) varying p for fixed m and ii) m and p both vary such that $m/p = \nu$, where $\nu > 0$ is a constant. Since p and m take only integer values, an exact analysis seems an arduous task. To circumvent this difficulty and in view of performing an approximate analysis, we let p and m be continuous variables. We can thus write the derivative of P_D with respect to p as

$$\frac{1}{(1-P_D)}\frac{\mathrm{d}P_D}{\mathrm{d}p} = \ln\left(1+\gamma-\gamma(1-P_F)^{1/mp}\right) + \gamma\frac{(1-P_F)^{1/mp}\ln(1-P_F)^{1/mp}}{1+\gamma-\gamma(1-P_F)^{1/mp}},$$

from which we obtain using the inequality $\ln z \geq 1 - 1/z$, $\frac{\mathrm{d}P_D}{\mathrm{d}p} > 0$. This in turn reveals that P_D increases with p for all γ and P_F, which is consistent with our intuition. The next immediate question of whether P_D is bounded as $p \to \infty$ is answered in the sequel.

We now focus on the second scenario. As such, noting that $m/p = \nu$, we can write derivative of P_D as a function of p to yield

$$\frac{1}{(1-P_D)}\frac{\mathrm{d}P_D}{\mathrm{d}p} = \ln\left(1+\gamma-\gamma(1-P_F)^{1/\nu p^2}\right) + 2\gamma\frac{(1-P_F)^{1/\nu p^2}\ln(1-P_F)^{1/\nu p^2}}{\left(1+\gamma-\gamma(1-P_F)^{1/\nu p^2}\right)}.$$

A careful inspection of the right hand expression reveals that it has only one stationary point. However, the direct evaluation of the stationary point based on the above expression does not yield any closed-form solution. Therefore, to gain insights into the p value which maximizes/minimizes P_D, in what follows,

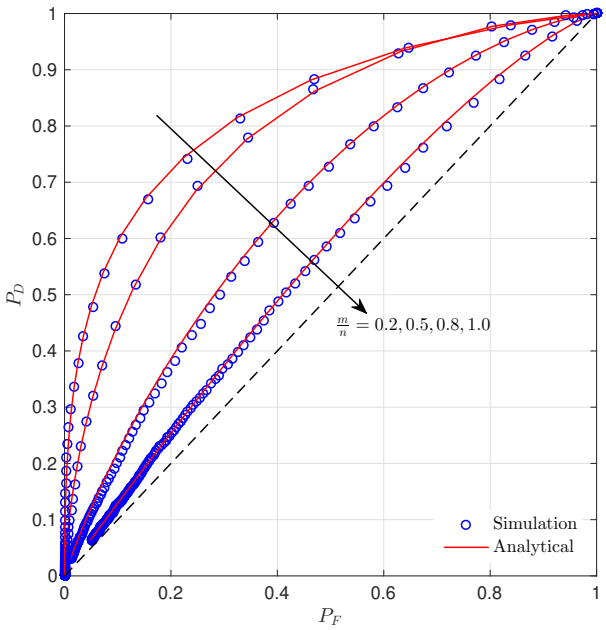

(a) For different m/n values with $m/p = 1$ and $n = 10$.

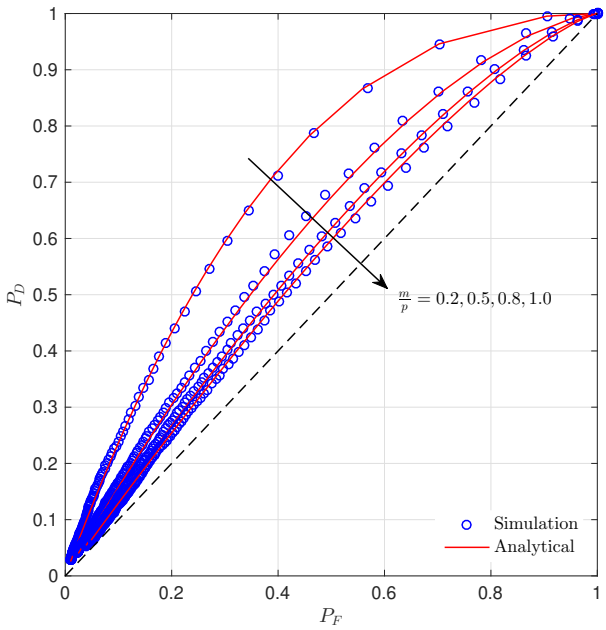

(b) For different m/p values with $m/n = 1$ and $p = 10$.

Fig. 5: P_D vs P_F for different (m, n, p) configurations with $\gamma = 5\,\text{dB}$.

we derive a tight bound for the stationary point. To this end, first we concentrate on the p values for which $\frac{\mathrm{d}P_D}{\mathrm{d}p} < 0$ for all γ and P_F. As such, we use the inequalities [56]

$$\ln(1+z) < \frac{z(z+2)}{2(z+1)}, \quad z > 0,$$

and $z \ln z < z(z-1)$, $z > 0$ to obtain

$$\begin{aligned}\ln\left(1+\gamma-\gamma(1-P_F)^{1/\nu p^2}\right) &+ 2\gamma\frac{(1-P_F)^{1/\nu p^2}\ln(1-P_F)^{1/\nu p^2}}{\left(1+\gamma-\gamma(1-P_F)^{1/\nu p^2}\right)} \\ &< \frac{\gamma(1-(1-P_F)^{1/\nu p^2})}{2\left(1+\gamma-\gamma(1-P_F)^{1/\nu p^2}\right)} \\ &\quad\times\left((\gamma+2)-(\gamma+4)(1-P_F)^{1/\nu p^2}\right).\end{aligned}$$

Therefore, $\frac{\mathrm{d}P_D}{\mathrm{d}p} < 0$ is strict in the regime where

$$p > \sqrt{\frac{-\ln(1-P_F)}{-\nu\ln\left(\frac{\gamma+2}{\gamma+4}\right)}}. \tag{27}$$

Again, using the inequalities [56], $\ln(1+z) > 2z/(2+z)$, $z > 0$ and $\ln z > (1-z)/\sqrt{z}$, $0 < z < 1$, we have

$$\begin{aligned}\ln\left(1+\gamma-\gamma(1-P_F)^{1/\nu p^2}\right) &+ 2\gamma\frac{(1-P_F)^{1/\nu p^2}\ln(1-P_F)^{1/\nu p^2}}{\left(1+\gamma-\gamma(1-P_F)^{1/\nu p^2}\right)} \\ &> 2\gamma(1-(1-P_F)^{1/\nu p^2}\left(\frac{1}{2+\gamma-\gamma(1-P_F)^{1/\nu p^2}}\right. \\ &\quad\left.-\frac{(1-P_F)^{1/2\nu p^2}}{1+\gamma-\gamma(1-P_F)^{1/\nu p^2}}\right).\end{aligned}$$

This in turn gives that $\frac{\mathrm{d}P_D}{\mathrm{d}p} > 0$ for

$$p < \sqrt{\frac{-\ln(1-P_F)}{-2\nu\ln\left(\frac{\gamma+1}{\gamma+2}\right)}}. \tag{28}$$

Thus, we conclude that P_D attains its maximum at $p = p^*$, where

$$\sqrt{\frac{-\ln(1-P_F)}{-2\nu\ln\left(\frac{\gamma+1}{\gamma+2}\right)}} < p^* < \sqrt{\frac{-\ln(1-P_F)}{-\nu\ln\left(\frac{\gamma+2}{\gamma+4}\right)}}. \tag{29}$$

Having obtained the upper and lower bounds on p^*, a good approximation of p^* can be written as[7]

$$p^* \approx \frac{1}{2}\left(\sqrt{\frac{-\ln(1-P_F)}{-\nu\ln\left(\frac{\gamma+2}{\gamma+4}\right)}} + \sqrt{\frac{-\ln(1-P_F)}{-2\nu\ln\left(\frac{\gamma+1}{\gamma+2}\right)}}\right). \tag{30}$$

[7]In general any convex combination of the upper and lower bounds can be a candidate for the p^*.

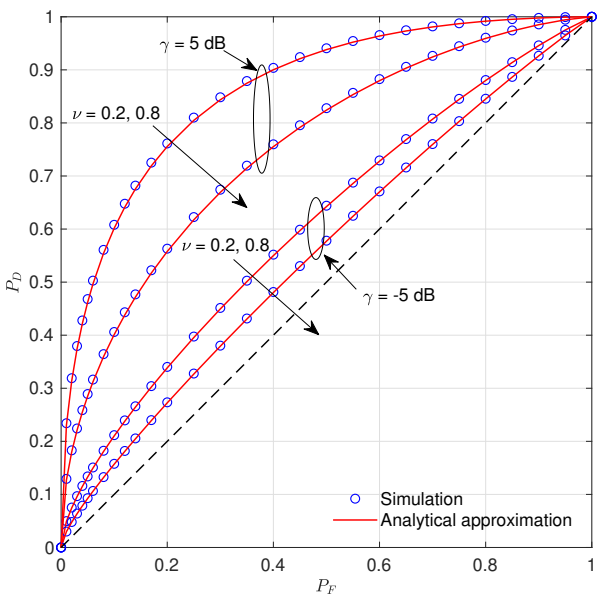

Fig. 6: P_D vs P_F for the optimal p and approximated p.

To further highlight the accuracy of the proposed approximation, in Fig. 6 we compare the optimal ROC profiles evaluated based on (30) and by numerically optimizing (26). As can be seen from the figure, the disparity between the proposed approximation and the exact optimal solution is insignificant. Therefore, when $m = n$, under the second scenario, we can choose p as per (30) for fixed P_F, γ, and ν in view of maximizing the detection probability.

The detection of a very weak signal embedded in noise is particularly challenging. In this respect, it is of paramount importance to understand the behavior of P_D as a function of SNR in the low SNR regime. To this end, we need to analytically characterize P_D around $\gamma = 0$, which is the focus of Corollary 13.

Corollary 13: As $\gamma \to 0$, for a fixed value of P_F, $P_D(\gamma)$ admits the following form

$$P_D(\gamma) = \begin{cases} P_F + pR_\epsilon(1-P_F)\gamma + o(\gamma) & \text{if } n > m \\ P_F + p\left[1-(1-P_F)^{1/mp}\right] \times (1-P_F)\,\gamma + o(\gamma) & \text{if } n = m \end{cases} \tag{31}$$

where

$$R_\epsilon(z) = z - \left(\frac{p+n}{p+m}\right)\frac{G(z)}{1+G(z)}z + \mathcal{K}(m,p,\alpha)\frac{(p+n)!}{(p+m+1)!} \times \left(\frac{G(z)}{1+G(z)}\right)^{m(m+\alpha+\beta+m)+1} \det\left[h_{i,j}\left(G(z)\right)\right] \tag{32}$$

with

$$h_{i,j}(z) = \begin{cases} \Psi_{1,j+1}(z) & i = 1;\ j = 1,2,\ldots,\alpha \\ \Psi_{i+1,j+1}(z) & i = 2,3,\ldots,\alpha;\ j = 1,2,\ldots,\alpha \end{cases}$$

and $G(z)$ being the inverse function of $F^{(\alpha)}_{\lambda_{\max}}(z;0)$. The proof simply follows by obtaining the Taylor expansion of the $P_D(\gamma)$ in the vicinity of $\gamma = 0$.

Let us now examine the factors affecting weak signal detection with the proposed scheme. Since the ROC curve for the case $n > m$ is too complicated, we confine ourselves to the scenario $m = n$. Moreover, as we have already seen, this scenario may result in the worst possible ROC and hence serves as a benchmark. Therefore, any improvement in this case will further enhance other ROC curves uniformly. Clearly, for very low SNR values, the most critical factor which determines the power is the coefficient of γ given by $p\left[1-(1-P_F)^{1/mp}\right](1-P_F)$. Since this coefficient depends on two parameters m and p for fixed P_F, we investigate the power profile when these parameters are related as follows: i) fixed m, p varies, ii) m and p both vary such that $m/p = k \in (0,1]$, and iii) m and p both vary such that $p-m$ is a constant. It is easy to show that under the above both options (ii) and (iii), the coefficient degrades when we increase both p and m. In contrast, when m is fixed, the coefficient gradually improves when we increase p. To show this, we rewrite the above coefficient, omitting the factor $(1-P_F)$, as a function of p to yield

$$a(p) = p\left[1-(1-P_F)^{1/mp}\right].$$

Now we treat p as a continuous variable and differentiate $a(p)$ over p to yield

$$\frac{\mathrm{d}}{\mathrm{d}p}a(p) = (1-P_F)^{1/mp}\ln(1-P_F)^{1/mp} + 1 - (1-P_F)^{1/mp}.$$

Noting the inequality, $\ln z \geq 1 - 1/z$, we can easily show that $\frac{\mathrm{d}}{\mathrm{d}p}a(p) \geq 0$ for all p, m. This in turn establishes that $a(p)$ is a non decreasing function of p. The next natural question is whether there exist an upper bound for $a(p)$ as p grows large. A simple limiting argument involving L'Hôpital's rule will then give

$$\lim_{p\to\infty} a(p) = -\frac{1}{m}\ln(1-P_F). \tag{33}$$

Therefore, we can conclude that a power enhancement is expected in the low SNR regime if we increase p for fixed m and P_F. In particular, in the low SNR regime (i.e., as $\gamma \to 0$), we have

$$P_F < P_D(\gamma) < P_F - \frac{(1-P_F)}{m}\ln(1-P_F)\,\gamma + o(\gamma). \tag{34}$$

To further asses the quality of the derived first order approximations, here we numerically evaluate the relative error between the exact $P_D(\gamma)$ and the corresponding first order expansions given in (31). To be precise, we define the relative error as

$$\text{RE} = \frac{P_D(\gamma) - P_D^{\text{f.o.}}(\gamma)}{P_D(\gamma)}$$

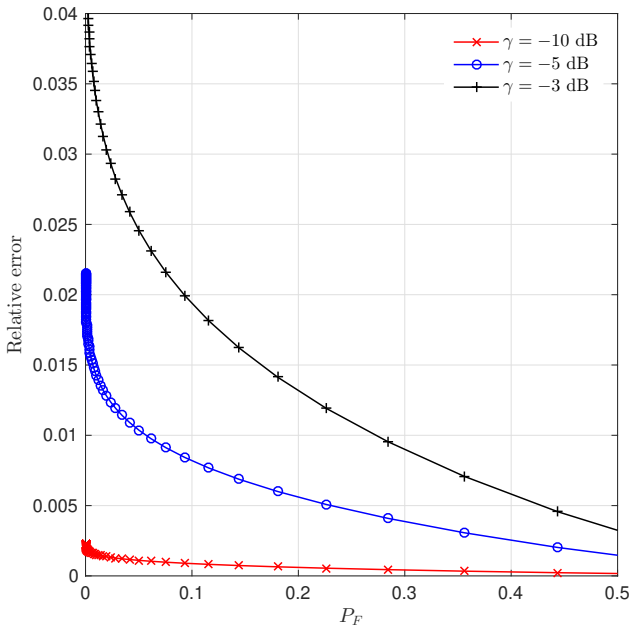

(a) For $m = p = 10$ and $n = 15$.

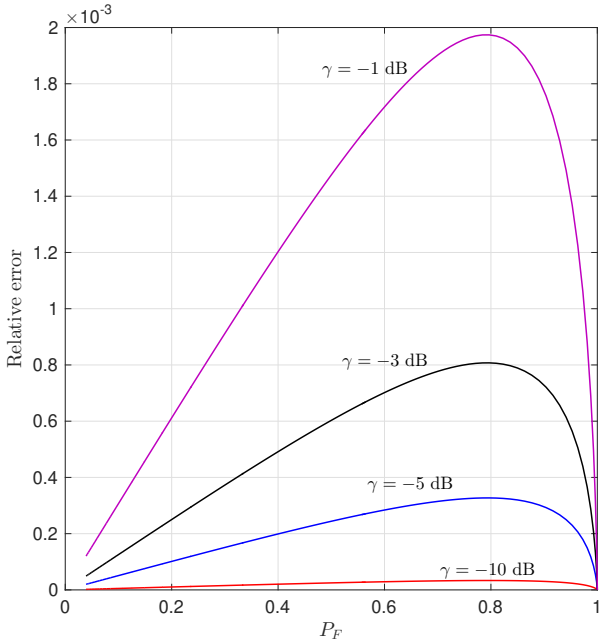

(b) For $m = n = 10$ and $p = 20$.

Fig. 7: Relative error vs P_F for small values of γ.

where $P_D^{\text{f.o.}}(\gamma)$ stands for the first order expansions give in (31). Figure 7a depicts the behavior of the relative error as a function of P_F for a set of small values of γ. The other parameters have been chosen as $m = n = 10$ and $p = 15$. Fig. 7a shows that the diminishing γ improves the relative error, which is anticipated. Fig. 7b shows the relative error versus P_F curve for a set of small values of γ when $m = n = 10$ and $p = 20$. Although we can observe the general trend of improving relative error with the diminishing γ, for a given γ, the relative error is maximized at a certain value of P_F. However, the analytical determination of this value seems an arduous task. The relative error improvement in the case of increasing p is depicted in Fig. 8. It is interesting to observe that the relative error does not deviate much from the corresponding asymptotic limit even for finite small values of p when γ is moderately low.

Having completed the finite-dimensional analysis, we now examine the ROC behavior in the asymptotic regime.

B. Asymptotic Analysis

Here we analyze the ROC profile in three important asymptotic regimes. In particular, we consider the following three regimes

1) As $m, n, p \to \infty$ such that α, β and γ are fixed,
2) As $p \to \infty$ such that $m = n$, and γ are fixed,
3) As $m, n, p, \gamma \to \infty$ such that $\frac{m}{n} \to 1$, $\frac{m}{p} \to c \in (0, 1]$, and $\frac{\gamma}{m} \to \theta \geq 0$.

Following Theorem 10, we can easily see that the maximum eigenvalue has no detection power in the first regime. Therefore, we now turn our attention to the second and third regimes. The asymptotic ROC pertaining to the second scenario can be obtained with the help of Corollary 12 as

$$P_D^{\text{Asyp}}(\gamma) = \lim_{p \to \infty} P_D(\gamma) = 1 - (1 - P_F)^{1 + \frac{\gamma}{m}}. \qquad (35)$$

It is noteworthy that this convergence is uniform in γ. Asymp-

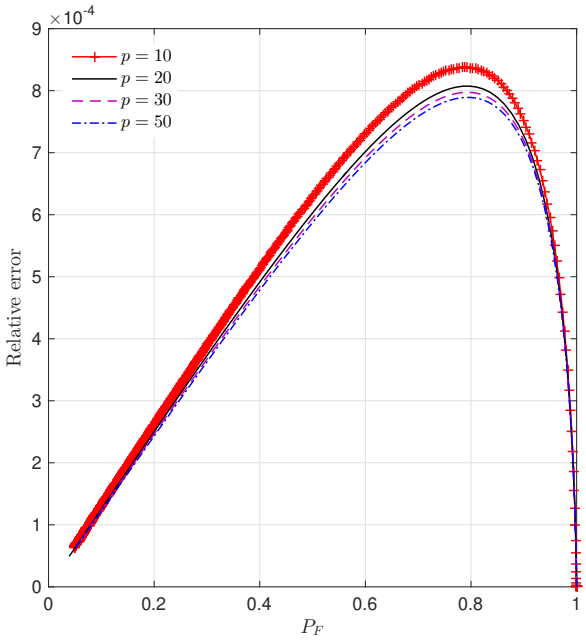

Fig. 8: Relative error vs P_F for different values of p with $m = n = 10$ and $\gamma = -3$ dB.

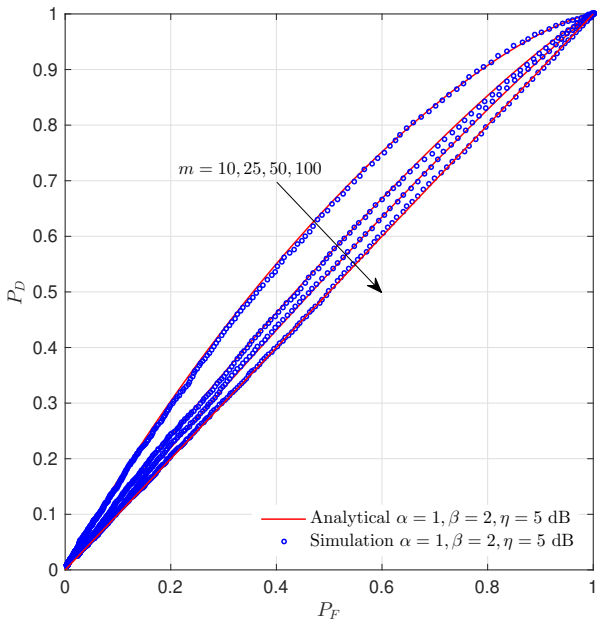

Fig. 9: P_D vs P_F as $m, n, p \to \infty$ such that $\alpha = n - m = 1$, $\beta = p - m = 2$, and $\gamma = 5$ dB are fixed.

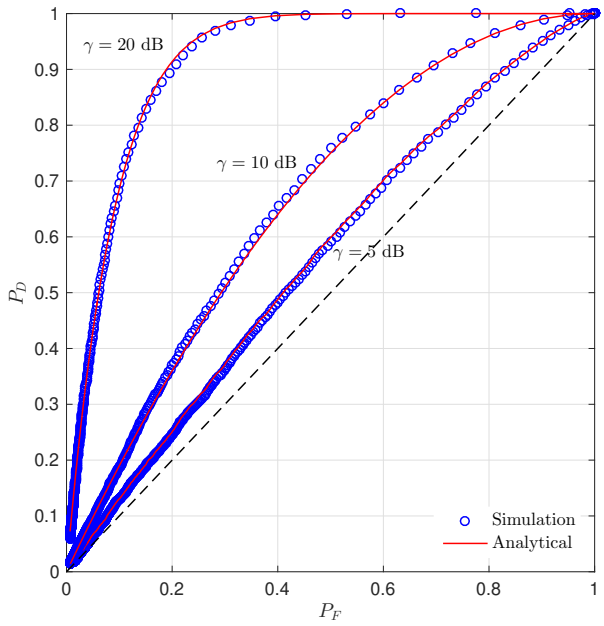

Fig. 10: Comparison of asymptotic and finite dimensional ROC profiles corresponding to Case 2 for different values of γ with $m = n = 10$ and $p = 25$.

totic ROC corresponding to the third regime, is given by the following corollary

Corollary 14: As $m, n, p, \gamma \to \infty$ such that $\frac{m}{n} \to 1$, $\frac{m}{p} \to c \in (0, 1]$, and $\frac{\gamma}{m} \to \theta \geq 0$, the ROC admits the following asymptotic limit

$$P_D^{\text{Asy}}(\theta) = 1 - (1 - P_F)^{1+\theta}. \tag{36}$$

Since the above asymptotic ROC profile is independent of c, this expression should be valid for $c = 0$ as well. Therefore, we can extend the domain of c such that $c \in [0, 1]$. Clearly, when $\theta = 0$ (γ does not scale with m), the maximum eigenvalue has no detection power in the high dimension. This is consistent with what has been reported in [39] on the power of the maximum eigenvalue below the phase transition. In contrast, when γ scales with m, in the high dimension, the maximum eigenvalue still retains its detection power. This valuable insight is of paramount importance in detecting signals over fading channels. For instance, for Rayleigh fading, which is the most commonly used statistical model in the literature, $\mathbf{h}$ takes the form $\mathbf{h} \sim \mathcal{CN}_m(\mathbf{0}, \mathbf{I}_m)$. Now, by invoking the strong law of large numbers, we obtain

$$\lim_{m \to \infty} \frac{||\mathbf{h}||^2}{m} \to 1, \quad \text{almost surely.} \tag{37}$$

This in turn shows that $\gamma \propto m$ as $m \to \infty$ for Rayleigh fading channels. This is a clear testament to the utility of our new asymptotic ROC profile given in Corollary 14 in wireless applications.

The above dynamics are depicted in Figs. 9, 10, and 11. In particular, Fig. 9 compares the analytical ROC profiles with the numerical results for an increasing sequence of m values when $\alpha = 1, \beta = 2$, and $\gamma = 5$ dB are fixed. As can be seen from the figure, when m increases the ROC profiles approach arbitrary closer to $P_D = P_F$ curve, thereby demonstrating the loss of the power of the test. This observation is consistent with what we have analytically shown related to the regime where α and β are fixed with $\gamma = 5$ dB. The effect of increasing p on the ROC profile is depicted in Fig. 10. The analytical curves are based on (35) and a close matching between the analytical and simulation results can be seen from the figure. This in turn shows us that that the analytical asymptotic result (as $p \to \infty$) derived in (35) serves as a good approximation to finite values of p as well. Finally, Fig. 11 compares the analytical asymptotic result for the third region where $m, n, p, \gamma \to \infty$ such that $\frac{m}{n} \to 1$, $\frac{m}{p} \to c \in (0, 1]$, and $\frac{\gamma}{m} \to \theta \geq 0$ with the simulation results. Again, closely matching two results reveal that our asymptotic analytical expression serves as a good approximation to the finite dimensional case as well. These results clearly indicate that, when γ scales with m, the maximum eigenvalue retains its detection power, whereas it looses the detection power when γ does not scale with m.

V. Conclusion

This paper investigates the signal detection problem in colored noise with unknown covariance matrix. The presence of a signal is detected by using the maximum generalized eigenvalue of the whitened sample covariance matrix. Equivalently, we need to determine the distribution of the maximum eigenvalue of the deformed JUE. To this end, we exploited the powerful orthogonal polynomial approach to develop a new c.d.f. expression for the maximum eigenvalue of the deformed JUE. Subsequently, we used it to determine the ROC of the detector. It turns out that, for a fixed SNR, when m (i.e.,

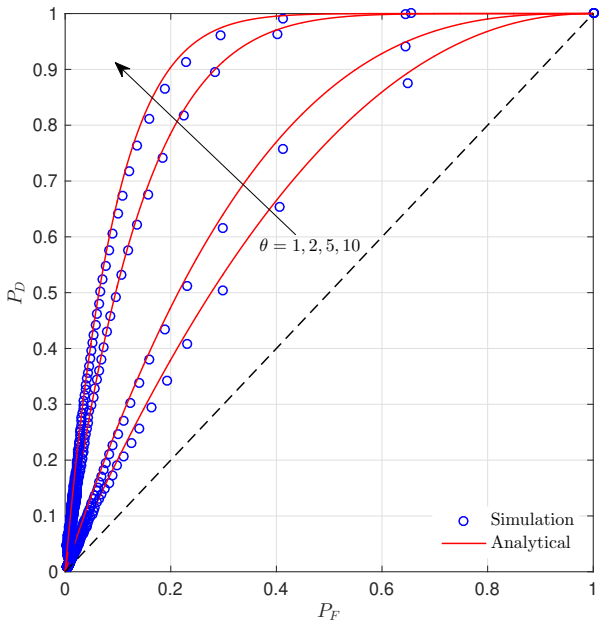

Fig. 11: Comparison of asymptotic and finite dimensional ROC profiles corresponding to Case 3 for different values of θ with $m = n = 25$ and $c = 1$.

the dimensionality of the detector), n (i.e., the number of noise-only samples), and p (i.e., the number of signal-plus-noise samples) increase over finite values such that $m = n$ and m/p is constant, we obtain an optimal ROC profile corresponding to specific m, n, and p values. In contrast, in the above setting, when m, p, and n increase asymptotically, the maximum eigenvalue gradually loses its detection power. This is not surprising, since under the above asymptotic setting, the detector operates below the so called phase transition where the maximum eigenvalue has no detection power. However, when the SNR scales with m, in the same asymptotic regime, the maximum eigenvalue retains its detection power. This fact is of paramount importance in detecting a signal in colored noise over fading channels (Rayleigh fading) where the SNR scales with the dimensionality of the system. Clearly, $m = n$ is the minimum requirement for the noise-only covariance matrix to be full rank (or nearly rank deficient). Therefore, some of the key results developed in this paper related to the setting $m = n$ shed some light into the regime where noise-only covariance matrix is nearly rank deficient. However, the analysis pertaining to the regime where the latter matrix is fully rank deficient remains an important open problem.

APPENDIX A
PROOF OF THE JOINT DENSITY OF THE EIGENVALUES

Following James [45], we can write the joint density of the eigenvalues of $\mathbf{W}_1\mathbf{W}_2^{-1}$ as

$$f(\lambda_1, \lambda_2, \ldots, \lambda_m) = \frac{\mathcal{K}_1(m,n,p)}{(1+\eta)^p} \prod_{j=1}^{m} \lambda_j^{p-m} \Delta_m^2(\boldsymbol{\lambda}) \times \int_{U(m)} \frac{1}{\det^{\alpha}[\mathbf{I}_m + \boldsymbol{\Sigma}_1^{-1}\mathbf{U}\boldsymbol{\Lambda}\mathbf{U}^{\dagger}]} \, \mathrm{d}\mathbf{U}. \tag{38}$$

where $\alpha = p + n$ and $\mathrm{d}\mathbf{U}$ is the invariant measure on the unitary group $U(m)$, normalized to make the total measure unity. Let us now focus on simplifying the above matrix integral. To this end, we use (12) to rewrite

$$\begin{aligned} &\int_{U(m)} \frac{1}{\det^{\alpha}[\mathbf{I}_m + \boldsymbol{\Sigma}_1^{-1}\mathbf{U}\boldsymbol{\Lambda}\mathbf{U}^{\dagger}]} \, \mathrm{d}\mathbf{U} \\ &\quad = \int_{U(m)} \frac{1}{\det^{\alpha}[\mathbf{I}_m + \mathbf{U}\boldsymbol{\Lambda}\mathbf{U}^{\dagger} - \mathbf{V}\boldsymbol{\Lambda}_{\eta}\mathbf{V}^{\dagger}\mathbf{U}\boldsymbol{\Lambda}\mathbf{U}^{\dagger}]} \, \mathrm{d}\mathbf{U} \\ &\quad = \int_{U(m)} \frac{1}{\det^{\alpha}[\mathbf{I}_m + \boldsymbol{\Lambda} - \mathbf{U}^{\dagger}\mathbf{V}\boldsymbol{\Lambda}_{\eta}\mathbf{V}^{\dagger}\mathbf{U}\boldsymbol{\Lambda}]} \, \mathrm{d}\mathbf{U} \end{aligned} \tag{39}$$

where $\boldsymbol{\Lambda}_{\eta} = \mathrm{diag}\,(\eta/(\eta+1), 0, \ldots, 0)$. Therefore, after some algebra, we obtain

$$\begin{aligned} &\int_{U(m)} \frac{1}{\det^{\alpha}[\mathbf{I}_m + \boldsymbol{\Sigma}_1^{-1}\mathbf{U}\boldsymbol{\Lambda}\mathbf{U}^{\dagger}]} \, \mathrm{d}\mathbf{U} \\ &\quad = \frac{1}{\det^{\alpha}[\mathbf{I}_m + \boldsymbol{\Lambda}]} \int_{U(m)} \frac{1}{\det^{\alpha}[\mathbf{I}_m - \mathbf{H}\boldsymbol{\Lambda}_{\eta}\mathbf{H}^{\dagger}\bar{\boldsymbol{\Lambda}}]} \mathrm{d}\mathbf{H} \end{aligned}$$

where $\bar{\boldsymbol{\Lambda}} = \boldsymbol{\Lambda}(\mathbf{I}_m + \boldsymbol{\Lambda})^{-1} = \mathrm{diag}\,(\bar{\lambda}_m, \ldots, \bar{\lambda}_1) = \mathrm{diag}\left(\frac{\lambda_m}{1+\lambda_m}, \ldots, \frac{\lambda_1}{1+\lambda_1}\right)$ and $\mathrm{d}\mathbf{H}$ is the invariant measure on the unitary group $U(m)$, normalized to make the total measure unity. Since $\boldsymbol{\Lambda}_{\eta}$ is rank one, we can further simplify the above matrix integral to yield

$$\begin{aligned} &\int_{U(m)} \frac{1}{\det^{\alpha}[\mathbf{I}_m + \boldsymbol{\Sigma}_1^{-1}\mathbf{U}\boldsymbol{\Lambda}\mathbf{U}^{\dagger}]} \, \mathrm{d}\mathbf{U} \\ &\quad = \frac{1}{\det^{\alpha}[\mathbf{I}_m + \boldsymbol{\Lambda}]} \int_{U(m)} \frac{1}{\left(1 - \mathrm{tr}\left(\mathbf{H}\boldsymbol{\Lambda}_{\eta}\mathbf{H}^{\dagger}\bar{\boldsymbol{\Lambda}}\right)\right)^{\alpha}} \, \mathrm{d}\mathbf{H}. \end{aligned}$$

Now it is worth observing that

$$\mathrm{tr}\left(\mathbf{H}\boldsymbol{\Lambda}_{\eta}\mathbf{H}^{\dagger}\bar{\boldsymbol{\Lambda}}\right) = \frac{\eta}{1+\eta}\mathbf{h}_1\bar{\boldsymbol{\Lambda}}\mathbf{h}_1^{\dagger} \leq \frac{\eta}{1+\eta}\frac{\lambda_m}{1+\lambda_m} < 1.$$

This in turn enables us to utilize the relation

$$\frac{1}{s^{\alpha}} = \frac{1}{\Gamma(\alpha)} \int_0^{\infty} y^{\alpha-1} \exp(-sy) \mathrm{d}y, \quad s > 0$$

to express the above matrix integral as

$$\begin{aligned} &\int_{U(m)} \frac{1}{\det^{\alpha}[\mathbf{I}_m + \boldsymbol{\Sigma}_1^{-1}\mathbf{U}\boldsymbol{\Lambda}\mathbf{U}^{\dagger}]} \, \mathrm{d}\mathbf{U} \\ &\quad = \frac{1}{\det^{\alpha}[\mathbf{I}_m + \boldsymbol{\Lambda}]} \frac{1}{\Gamma(\alpha)} \int_0^{\infty} y^{\alpha-1} \exp(-y)\Phi(y) \mathrm{d}y \end{aligned} \tag{40}$$

where

$$\Phi(y) = \int_{U(m)} \exp\left\{y\mathrm{tr}\left(\mathbf{H}\boldsymbol{\Lambda}_{\eta}\mathbf{H}^{\dagger}\bar{\boldsymbol{\Lambda}}\right)\right\} \mathrm{d}\mathbf{H}$$

and we have taken the liberty of changing the order of integration. Noting the fact that

$$\exp\left\{y\mathrm{tr}\left(\mathbf{H}\boldsymbol{\Lambda}_{\eta}\mathbf{H}^{\dagger}\bar{\boldsymbol{\Lambda}}\right)\right\} = {}_0\widetilde{F}_0(y\mathbf{H}\boldsymbol{\Lambda}_{\eta}\mathbf{H}^{\dagger}\bar{\boldsymbol{\Lambda}}),$$

we may use the splitting formula [45, eq. 92] to yield

$$\Phi(y) = \int_{U(m)} {}_0\widetilde{F}_0(y\mathbf{H}\mathbf{\Lambda}_\eta\mathbf{H}^\dagger\bar{\mathbf{\Lambda}})\mathrm{d}\mathbf{H} = {}_0\widetilde{F}_0\left(y\mathbf{\Lambda}_\eta, \bar{\mathbf{\Lambda}}\right).$$

Following [38], we can show that

$${}_0\widetilde{F}_0\left(y\mathbf{\Lambda}_\eta, \bar{\mathbf{\Lambda}}\right) = \Gamma(m)\left(\frac{1+\eta}{\eta}\right)^{m-1} y^{1-m} \times \sum_{k=1}^{m} \frac{\exp\left(\frac{\eta\bar{\lambda}_k}{1+\eta}y\right)}{\prod_{\substack{j=1\\ j\neq k}}(\bar{\lambda}_k - \bar{\lambda}_j)}$$

from which we obtain upon substituting into (40) with some algebra

$$\int_{U(m)} \frac{1}{\det^\alpha[\mathbf{I}_m + \mathbf{\Sigma}_1^{-1}\mathbf{U}\mathbf{\Lambda}\mathbf{U}^\dagger]}\,\mathrm{d}\mathbf{U} = \frac{\Gamma(\alpha-m+1)\Gamma(m)}{\Gamma(\alpha)}\left(\frac{1+\eta}{\eta}\right)^{m-1}\frac{1}{\prod_{j=1}^m(1+\lambda_j)^\alpha} \times \sum_{k=1}^{m}\frac{1}{\prod_{\substack{j=1\\ j\neq k}}(\bar{\lambda}_k-\bar{\lambda}_j)}\frac{1}{\left(1-\frac{\eta\bar{\lambda}_k}{1+\eta}\right)^{\alpha-m+1}}. \quad (41)$$

Finally, using (41) in (38) with some algebraic manipulation we obtain (13), which concludes the proof.

APPENDIX B
PROOF OF THE C.D.F. OF THE MAXIMUM EIGENVALUE

By exploiting the symmetry, the ordered region of integration in (17) can be rearranged as an unordered region to yield

$$\Pr(x_{\max}\leq t) = \frac{\mathcal{K}(m,n,p)}{m!\,\eta^{m-1}(1+\eta)^{p+1-m}} \times \sum_{k=1}^{m}\int_{[0,t]^m}\frac{\Delta_m^2(\mathbf{x})\prod_{j=1}^m x_j^{p-m}(1-x_j)^{n-m}}{\prod_{\substack{j=1\\ j\neq k}}^m(x_i-x_j)\left(1-\frac{\eta}{1+\eta}x_k\right)^{p+n+1-m}}\,\mathrm{d}\mathbf{x} \quad (42)$$

where $[0,t]^m = [0,t]\times[0,t]\times\ldots\times[0,t]$ with $\times$ denoting the Cartesian product. Since each term in the above summation contributes the same amount to the final solution, it can be further simplified as

$$\Pr(x_{\max}\leq\ t) = \frac{\mathcal{K}}{(m-1)!}\int_{[0,t]^m}\frac{\Delta_m^2(\mathbf{x})\prod_{j=1}^m x_j^\beta(1-x_j)^\alpha}{\prod_{j=2}^m(x_1-x_j)\left(1-\frac{\eta}{1+\eta}x_1\right)^\gamma}\,\mathrm{d}\mathbf{x}$$

where

$$\mathcal{K} = \frac{\mathcal{K}(m,n,p)}{\eta^{m-1}(1+\eta)^{p+1-m}}.$$

Here we have relabeled the variables as $\alpha = n-m$, $\beta = p-m$ and $\gamma = m+\alpha+\beta+1$ for notational concision. To facilitate further analysis, let us decompose the Vandermonde determinant as

$$\Delta_m(\mathbf{x}) = \prod_{j=2}^m(x_1-x_j)\Delta_{m-1}(\mathbf{x})$$

and relabel the variables $x_1 = y$ and $x_j = z_{j-1}$, $j = 2,3,...,m$, to obtain

$$\Pr(x_{\max}\leq t) = \frac{\mathcal{K}}{(m-1)!}\int_{[0,t]^m}\frac{y^\beta(1-y)^\alpha}{\left(1-\frac{\eta}{1+\eta}y\right)^\gamma}\prod_{j=1}^{m-1}z_j^\beta(1-z_j)^\alpha(y-z_j) \times\Delta_{m-1}^2(\mathbf{z})\,\mathrm{d}\mathbf{z}\,\mathrm{d}y \quad (43)$$

where $\mathbf{z}\in\mathbb{R}^{m-1}$. Now we apply the variable transformations $y = tx$ and $z_j = ts_j$, $j = 1,2,...,m-1$, to make the region of integration independent of t in (43). Consequently, after some algebraic manipulations, we have

$$\Pr(x_{\max}\leq t) = \frac{\mathcal{K}}{(m-1)!}t^{m(\beta+m-1)+1} \times\int_0^1\frac{x^\beta(1-tx)^\alpha}{\left(1-\frac{\eta t}{1+\eta}x\right)^\gamma}\mathcal{Q}_{m-1}(\beta,\alpha,x,t)\mathrm{d}x \quad (44)$$

where

$$\mathcal{Q}_m(\beta,\alpha,x,t) = \int_{[0,1]^m}\prod_{j=1}^m s_j^\beta(1-ts_j)^\alpha(x-s_j)\Delta_m^2(\mathbf{s})\mathrm{d}\mathbf{s}. \quad (45)$$

Following Appendix C, we can solve the above multidimensional integral to yield

$$\mathcal{Q}_m(\beta,\alpha,x,t) = \tilde{\mathcal{C}}_{(0,\beta,m)}\frac{t^{\alpha m}}{2^{m(\alpha+\beta+m+1)+\frac{\alpha}{2}(\alpha+1)}\prod_{j=1}^{\alpha-1}j!}\frac{1}{(1-xt)^\alpha} \times\det\left[P_{m+i-1}^{(0,\beta)}\left(h_{\frac{1}{x}}\right)\quad(m+i+\beta)_{j-2} \times P_{m+i-j+1}^{(j-2,\beta+j-2)}(h_t)\right]_{\substack{i=1,2,\ldots,\alpha+1\\ j=2,3,\ldots,\alpha+1}} \quad (46)$$

where

$$\tilde{\mathcal{C}}_{(0,\beta,m)} = \mathcal{C}_{(0,\beta,m)} \times\prod_{j=1}^{\alpha+1}2^{m+j-1}\frac{(m+j-1)!\,(m+\beta+j-1)!}{(2m+2j+\beta-2)!},$$

$$\mathcal{C}_{(0,\beta,m)} = 2^{m(\beta+m)}\prod_{j=0}^{m-1}\frac{(j)!\,(j+1)!\,(\beta+j)!}{(\beta+m+j)!},$$

and $h_t = \frac{2}{t}-1$. Using (46) in (44) with some algebraic manipulation we have

$$\Pr(x_{\max}\leq t) = \frac{\mathcal{K}\tilde{\mathcal{C}}_{(0,\beta,m-1)}t^{m(\alpha+\beta+m-1)+1}}{(m-1)!\,2^{(m-1)(\alpha+\beta+m)+\frac{\alpha}{2}(\alpha+1)}\prod_{j=1}^{\alpha-1}j!} \times\int_0^1\frac{x^\beta}{\left(1-\frac{\eta t}{1+\eta}x\right)^\gamma} \times\det\left[P_{m+i-2}^{(0,\beta)}(2x-1)\quad\Psi_{i,j}\left(\frac{t}{1-t}\right)\right]_{\substack{i=1,2,\ldots,\alpha+1\\ j=2,3,\ldots,\alpha+1}}\mathrm{d}x. \quad (47)$$

Having observed that only the first column of the determinant in the integrand depends on x, we can rewrite the above integral as

$$\begin{aligned}&\Pr(x_{\max}\le t)\\&=\frac{\mathcal{K}\tilde{\mathcal{C}}_{(0,\beta,m-1)}t^{m(\alpha+\beta+m-1)+1}}{(m-1)!\,2^{(m-1)(\alpha+\beta+m)+\frac{\alpha}{2}(\alpha+1)}\prod_{j=1}^{\alpha-1}j!}\\&\quad\times\det\left[\int_0^1\frac{x^\beta}{\left(1-\frac{\eta t}{1+\eta}x\right)^\gamma}P_{m+i-2}^{(0,\beta)}(2x-1)\mathrm{d}x\right.\\&\qquad\left.\Psi_{i,j}\left(\frac{t}{1-t}\right)\right]_{\substack{i=1,2,\ldots,\alpha+1\\j=2,3,\ldots,\alpha+1}}.\end{aligned}\tag{48}$$

For clarity, let us focus on the integral in the above equation. In this respect, we may use the relation (10) followed by the variable transformation $y=1-x$ to arrive at

$$\begin{aligned}&\int_0^1\frac{x^\beta}{\left(1-\frac{\eta t}{1+\eta}x\right)^\gamma}P_{m+i-1}^{(0,\beta)}(2x-1)\mathrm{d}x\\&=\frac{1}{\left(1-\frac{\eta t}{1+\eta}\right)^\gamma}\int_0^1\frac{(1-y)^\beta}{\left(1+\frac{\eta t}{1+\eta(1-t)}y\right)^\gamma}\\&\qquad\times{}_2F_1(-m-i+2,m+\beta+i-1\\&\qquad;1;y)\ \mathrm{d}y,\end{aligned}$$

which can be solved using [57, eq. 399.6] to obtain

$$\begin{aligned}&\int_0^1\frac{x^\beta}{\left(1-\frac{\eta t}{1+\eta}x\right)^\gamma}P_{m+i-1}^{(0,\beta)}(2x-1)\mathrm{d}x\\&=\frac{\Gamma(\beta+1)}{\Gamma(\beta+m+i)\Gamma(3-m-i)}\\&\qquad\times{}_3F_2\left(\beta+1,\gamma,1;\beta+m+i,3-m-i;\frac{\eta t}{1+\eta}\right).\end{aligned}$$

To facilitate further analysis, noting that $\frac{\eta t}{1+\eta}<1$, we may replace the hypergeometric function with its equivalent infinite series expansion to yield

$$\begin{aligned}&\int_0^1\frac{x^\beta}{\left(1-\frac{\eta t}{1+\eta}x\right)^\gamma}P_{m+i-1}^{(0,\beta)}(2x-1)\mathrm{d}x\\&=\frac{\Gamma(\beta+1)}{\Gamma(\beta+m+i)\Gamma(3-m-i)}\\&\qquad\times\sum_{k=0}^{\infty}\frac{(\beta+1)_k(\gamma)_k(1)_k}{k!\,(\beta+m+i)_k(3-m-i)_k}\left(\frac{\eta t}{1+\eta}\right)^k.\end{aligned}$$

Since the Gamma function has poles at negative integer values including zero, the above series is nonzero if the argument of $\Gamma(3-m-i+k)=\Gamma(3-m-i)\,(3-m-i)_k$ is a positive integer. To this end, k should satisfy the inequality $k\ge m+i-2$. Therefore, by relabeling summation index k as $j=k-m-i+2$, we obtain

$$\begin{aligned}&\int_0^1\frac{x^\beta}{\left(1-\frac{\eta t}{1+\eta}x\right)^\gamma}P_{m+i-2}^{(0,\beta)}(2x-1)\mathrm{d}x\\&=\frac{\Gamma(\beta+1)}{\Gamma(\beta+m+i)}\sum_{j=0}^{\infty}\frac{(\beta+1)_{m+i+j-2}(\gamma)_{m+i+j-2}}{j!\,(\beta+m+i)_{m+i+j-2}}\\&\qquad\times\frac{(1)_{m+i+j-2}}{(m+i+j-2)!}\left(\frac{\eta t}{1+\eta}\right)^{m+i+j-2}.\end{aligned}$$

The above infinite series can be rearranged by using the addition formula $(a)_{n+k}=(a)_n(a+n)_k$ with some algebraic manipulations to yield

$$\begin{aligned}&\int_0^1\frac{x^\beta}{\left(1-\frac{\eta t}{1+\eta}x\right)^\gamma}P_{m+i-2}^{(0,\beta)}(2x-1)\mathrm{d}x\\&\quad=\frac{\Gamma(a_i)\Gamma(b_i)}{\Gamma(\gamma)\Gamma(c_i)}\left(\frac{\eta t}{1+\eta}\right)^{m+i-2}{}_2F_1\left(a_i,b_i;c_i;\frac{\eta t}{1+\eta}\right),\end{aligned}\tag{49}$$

where $a_i=\beta+m+i-1$, $b_i=\gamma+m+i-2$, and $c_i=\beta+2m+2i-2$. Now we substitute (49) into (48) followed by some algebraic manipulations to obtain the c.d.f. of $x_{\max}$ as

$$\begin{aligned}&\Pr(x_{\max}\le t)\\&=\frac{t^{m(\alpha+\beta+m)}}{(p-1)!\,(1+\eta)^p}\left(\prod_{j=0}^{\alpha-1}\frac{(p+m+j-1)!}{(p+m+2j)!}\right)\\&\quad\times\det\left[\frac{\Gamma(a_i)\Gamma(b_i)}{\Gamma(c_i)}\left(\frac{\eta t}{1+\eta}\right)^{i-1}{}_2F_1\left(a_i,b_i;c_i;\frac{\eta t}{1+\eta}\right)\right.\\&\qquad\left.\times\ \Psi_{i,j}\left(\frac{t}{1-t}\right)\right]_{\substack{i=1,2,\ldots,\alpha+1\\j=2,3,\ldots,\alpha+1}}.\end{aligned}\tag{50}$$

Now (18) with $\Phi(t,\eta)$ given by (19) follows by transforming the variable $x_{\max}$ to $\lambda_{\max}$ using the functional relation $\lambda_{\max}=x_{\max}/(1-x_{\max})$. Finally, noting that c_i-b_i is a negative integer, we may use the hypergeometric transformation [58, eq. 15.3.4],

$${}_2F_1(a,b,c,z)=(1-z)^{-a}\,{}_2F_1\left(a,c-b,c,\frac{z}{z-1}\right),\tag{51}$$

to arrive at the finite series form of $\Phi(t,\eta)$, thereby concluding the proof.

APPENDIX C

Let us change the region of integration in (45) from $[0,1]^m$ to $[-1,1]^m$ by using the variable transformation $s_j=\frac{1+z_j}{2}$, $j=1,2,...,m$, to yield

$$\mathcal{Q}_m(\beta,\alpha,x,t)=\frac{t^{\alpha m}}{2^{m(m+\beta+\alpha+1)}}\mathcal{R}_m(\beta,\alpha,x,t)\tag{52}$$

where

$$\begin{aligned}\mathcal{R}_m(\beta,\alpha,x,t)=\int_{[-1,1]^m}\prod_{j=1}^{m}(1+z_j)^\beta(h_t-z_j)^\alpha\left(h_{\frac{1}{x}}-z_j\right)\\\times\Delta_m^2(\mathbf{z})\ \mathrm{d}\mathbf{z},\end{aligned}\tag{53}$$

with $h_t = \frac{2}{t} - 1$ and $\mathbf{z} \in \mathbb{R}^m$. Our strategy is to start with a related integral given in [43, eqs. 22.4.2, 22.4.11] as

$$\begin{aligned}&\int_{[-1,1]^m} \prod_{j=1}^{m} (1+z_j)^{\beta} \prod_{i=1}^{\alpha+1} (r_i - z_j) \Delta_m^2(\mathbf{z})\, \mathrm{d}\mathbf{z} \\ &\quad = \mathcal{C}_{(0,\beta,m)} \Delta_{\alpha+1}^{-1}(\mathbf{r}) \det\left[C_{m+i-1}(r_j)\right]_{i,j=1,2,\ldots,\alpha+1}\end{aligned} \tag{54}$$

where

$$\mathcal{C}_{(0,\beta,m)} = 2^{m(\beta+m)} \prod_{j=0}^{m-1} \frac{j!\,(j+1)!\,(\beta+j)!}{(\beta+m+j)!}$$

and $C_k(x)$ are monic polynomials orthogonal with respect to the weight $(1+x)^{\beta}$, over $-1 \le x \le 1$. Since Jacobi polynomials are orthogonal with respect to the preceding weight, we use $C_k(x) = 2^k \frac{(k+\beta)!(k)!}{(2k+\beta)!} P_k^{(0,\beta)}(x)$ in (54) to obtain

$$\begin{aligned}&\int_{[-1,1]^m} \prod_{j=1}^{m} (1+z_j)^{\beta} \prod_{i=1}^{\alpha+1} (r_i - z_j) \Delta_m^2(\mathbf{z})\, \mathrm{d}\mathbf{z} \\ &\qquad = \frac{\tilde{\mathcal{C}}_{(0,\beta,m)}}{\Delta_{\alpha+1}(\mathbf{r})} \det\left[P_{m+i-1}^{(0,\beta)}(r_j)\right]_{i,j=1,2,\ldots,\alpha+1}\end{aligned} \tag{55}$$

where

$$\begin{aligned}\tilde{\mathcal{C}}_{(0,\beta,m)} &= \mathcal{C}_{(0,\beta,m)} \\ &\quad \times \prod_{j=1}^{\alpha+1} \frac{2^{m+j-1}(m+j-1)!\,(m+\beta+j-1)!}{(2m+2j+\beta-2)!}.\end{aligned}$$

In the above, r_is are generally distinct parameters. Nevertheless, if we choose r_i such that

$$r_i = \begin{cases} h_{\frac{1}{x}} & \text{if } i = 1 \\ h_t & \text{if } i = 2,3,\ldots,\alpha+1, \end{cases}$$

then the left side of (55) coincides with the multidimensional integral of our interest in (53). Under the above parameter selection, however, the right side of (55) takes the indeterminate form $0/0$. Therefore, we have to evaluate following limit:

$$\begin{aligned}&\mathcal{R}_m(\beta,\alpha,x,t) \\ &= \tilde{\mathcal{C}}_{(0,\beta,m)} \lim_{\substack{r_1 \to h_{\frac{1}{x}} \\ r_2,r_3,\ldots,r_{\alpha+1} \to h_t}} \frac{\det\left[P_{m+i-1}^{(0,\beta)}(r_j)\right]_{i,j=1,2,\ldots,\alpha+1}}{\Delta_{\alpha+1}(\mathbf{r})}.\end{aligned} \tag{56}$$

To this end, following Khatri [53], we write

$$\begin{aligned}&\lim_{\substack{r_1 \to h_{\frac{1}{x}} \\ r_2,r_3,\ldots,r_{\alpha+1} \to h_t}} \frac{\det\left[P_{m+i-1}^{(0,\beta)}(r_j)\right]_{i,j=1,2,\ldots,\alpha+1}}{\Delta_{\alpha+1}(\mathbf{r})} \\ &= \frac{\det\left[P_{m+i-1}^{(0,\beta)}(h_{\frac{1}{x}}) \quad \frac{\mathrm{d}^{j-2}}{\mathrm{d}h_t^{j-2}} P_{m+i-1}^{(0,\beta)}(h_t)\right]_{\substack{i=1,2,\ldots,\alpha+1 \\ j=2,3,\ldots,\alpha+1}}}{\det\left[h_{\frac{1}{x}}^{i-1} \quad \frac{\mathrm{d}^{j-2}}{\mathrm{d}h_t^{j-2}} h_t^{i-1}\right]_{\substack{i=1,2,\ldots,\alpha+1 \\ j=2,3,\ldots,\alpha+1}}}.\end{aligned} \tag{57}$$

Now the determinant in the denominator of (57) simplifies to

$$\det\left[h_{\frac{1}{x}}^{i-1} \quad \frac{\mathrm{d}^{j-2}}{\mathrm{d}h_t^{j-2}} h_t^{i-1}\right]_{\substack{i=1,2,\ldots,\alpha+1 \\ j=2,3,\ldots,\alpha+1}} = \prod_{j=1}^{\alpha-1} j!\,(h_t - h_{\frac{1}{x}})^{\alpha}.$$

The numerator can be rewritten with the help of (11) as

$$\begin{aligned}&\det\left[P_{m+i-1}^{(0,\beta)}(h_{\frac{1}{x}}) \quad \frac{\mathrm{d}^{j-2}}{\mathrm{d}h_t^{j-2}} P_{m+i-1}^{(0,\beta)}(h_t)\right]_{\substack{i=1,2,\ldots,\alpha+1 \\ j=2,3,\ldots,\alpha+1}} \\ &= 2^{-\frac{\alpha}{2}(\alpha-1)} \det\Big[P_{m+i-1}^{(0,\beta)}(h_{\frac{1}{x}}) \qquad (m+\beta+i)_{j-2} \\ &\qquad\qquad \times P_{m+i-j+1}^{(j-2,\beta+j-2)}(h_t)\Big]_{\substack{i=1,2,\ldots,\alpha+1 \\ j=2,3,\ldots,\alpha+1}}.\end{aligned}$$

Substituting the above two expression into (57) and then the result into (56) gives

$$\begin{aligned}&\mathcal{R}_m(\beta,\alpha,x,t) \\ &= \tilde{\mathcal{C}}_{(0,\beta,m)} \frac{t^{\alpha}}{2^{\frac{\alpha}{2}(\alpha+1)} \prod_{j=1}^{\alpha-1} j!\,(1-xt)^{\alpha}} \\ &\quad \times \det\Big[P_{m+i-1}^{(0,\beta)}\left(h_{\frac{1}{x}}\right) \qquad (m+i+\beta)_{j-2} \\ &\qquad\qquad \times P_{m+i-j+1}^{(j-2,\beta+j-2)}(h_t)\Big]_{\substack{i=1,2,\ldots,\alpha+1 \\ j=2,3,\ldots,\alpha+1}}.\end{aligned}$$

APPENDIX D
PROOF OF THE MICROSCOPIC LIMIT OF THE C.D.F. OF THE MAXIMUM EIGENVALUE

Let us rewrite (50), keeping in mind $\alpha = n-m$, $\beta = p-m$, and $\gamma = m+\alpha+\beta+1$, as

$$\begin{aligned}&\Pr(x_{\max} \le t) \\ &= t^{m(\alpha+\beta+m)} \left(\prod_{j=0}^{\alpha-1} \frac{(\beta+2m+j-1)!}{(\beta+2m+2j)!}\right) \\ &\quad \times \det\Big[\mathcal{P}_i(m,\alpha,\beta,\eta,t) \qquad (m+i+\beta-1)_{j-2} \\ &\qquad\qquad \times P_{m+i-j}^{(j-2,\beta+j-2)}\left(\frac{2}{t}-1\right)\Big]_{\substack{i=1,2,\ldots,\alpha+1 \\ j=2,3,\ldots,\alpha+1}}\end{aligned} \tag{58}$$

where

$$\begin{aligned}&\mathcal{P}_i(m,\alpha,\beta,\eta,t) \\ &= \frac{\Gamma(\alpha+\beta+2m+i-1)\Gamma(\beta+m+i-1)}{\Gamma(\beta+2m+2i-2)\Gamma(m+\beta)(1+\eta)^{m+\beta}} \left(\frac{\eta t}{1+\eta}\right)^{i-1} \\ &\quad \times {}_2F_1\Big(\beta+m+i-1, \alpha+\beta+2m+i-1; \beta+2m+2i \\ &\qquad\qquad - 2; \frac{\eta t}{1+\eta}\Big).\end{aligned}$$

Following (10), the Jacobi polynomial $P_{m+i-j}^{(j-2,\beta+j-2)}(2/t-1)$ can be written as

$$\begin{aligned}&P_{m+i-j}^{(j-2,\beta+j-2)}\left(\frac{2}{t}-1\right) \\ &= \frac{(j-1)_{m+i-j}}{(m+i-j)!} \\ &\quad \times {}_2F_1\Big(-(m+i-j), m+\beta+i+j-3; j-1; 1-\frac{1}{t}\Big),\end{aligned} \tag{59}$$

from which we obtain

$$P_{m+i-j}^{(j-2,\beta+j-2)}\left(\frac{2}{t}-1\right) = \frac{(m+i-2)!}{(m+i-j)!\,(j-2)!}\sum_{k_j=0}^{m+i-j}\frac{(-(m+i-j))_{k_j}}{k_j!\,(j-1)_{k_j}} \times (m+\beta+i+j-3)_{k_j}\left(1-\frac{1}{t}\right)^{k_j}.$$

To facilitate further analysis, we need to eliminate the dependence of summation upper limit on i. To this end, we decompose the two Pochhammer symbols in the numerator of the above summation as

$$(-(m+i-j))_{k_j} = \frac{(-(m+\alpha-j+1))_{k_j}(m+i-j)!}{(m+\alpha-j+1)!} \times (m+i-j-k_j+1)_{\alpha-i+1}$$

and

$$(m+\beta+i+j-3)_{k_j} = \frac{(m+\beta+j-2))_{k_j}(m+\beta+j-3)!}{(m+\beta+i+j-4)!} \times (m+\beta+j+k_j-2)_{i-1}.$$

Therefore, we obtain

$$(m+i+\beta-1)_{j-2}P_{m+i-j}^{(j-2,\beta+j-2)}\left(\frac{2}{t}-1\right) = \frac{(m+i-2)!\,(m+\beta+j-3)!\,(j-2)!\,(m+i-j)!}{(m+i+\beta-2)!\,(m+i-j)!\,(j-2)!\,(m+\alpha-j+1)!} \times \mathcal{S}_{k_j}(t)\mathcal{U}_{i,j}(m,\alpha,\beta) \quad (60)$$

where

$$\mathcal{S}_{k_j}(t) = \sum_{k_j=0}^{m+\alpha-j+1}\frac{(-(m+\alpha-j+1))_{k_j}}{k_j!\,(j+k_j-2)!} \times (m+\beta+j-2)_{k_j}\left(1-\frac{1}{t}\right)^{k_j}$$

and

$$\mathcal{U}_{i,j}(m,\alpha,\beta) = (m+\beta+j+k_j-2)_{i-1} \times (m+i-j-k_j+1)_{\alpha-i+1}. \quad (61)$$

Now we substitute (60) into (58) with some algebraic manipulation to yield

$$\Pr(x_{\max}\le t) = \left(\prod_{j=0}^{\alpha-1}\frac{\mathcal{S}_{k_{j+2}}(t)(\beta+2m+j-1)!\,(m+\beta+j-1)!}{(\beta+2m+2j)!\,(m+\alpha-j-1)!}\right) \times t^{m(\alpha+\beta+m)}\det\left[\mathcal{P}_i(m,\alpha,\beta,\eta,t)\quad\frac{(m+i-2)!}{(m+\beta+i-2)!} \times \mathcal{U}_{i,j}(m,\alpha,\beta)\right]_{\substack{i=1,2,\ldots,\alpha+1\\ j=2,3,\ldots,\alpha+1}},$$

from which we obtain after some rearrangements

$$\Pr(x_{\max}\le t) = t^{m(\alpha+\beta+m)}\left(\frac{(m-1)!}{(m+\alpha+\beta-1)!}\right) \times\left(\prod_{j=0}^{\alpha-1}\frac{\mathcal{S}_{k_{j+2}}(t)(\beta+2m+j-1)!}{(\beta+2m+2j)!}\right) \times\det\left[\frac{(m+\beta+i-2)!}{(m+i-2)!}\mathcal{P}_i(m,\alpha,\beta,\eta,t) \mathcal{U}_{i,j}(m,\alpha,\beta)\right]_{\substack{i=1,2,\ldots,\alpha+1\\ j=2,3,\ldots,\alpha+1}}.$$

For convenience, let us rewrite the above equation as

$$\Pr(x_{\max}\le t) = t^{m(\alpha+\beta+m)}\left(\prod_{j=0}^{\alpha-1}\frac{\mathcal{S}_{k_{j+2}}(t)(\beta+2m+j-1)!}{(\beta+2m+2j)!}\right) \times\det\left[\mathcal{V}_i(m,\alpha,\beta,\eta,t) \mathcal{U}_{i,j}(m,\alpha,\beta)\right]_{\substack{i=1,2,\ldots,\alpha+1\\ j=2,3,\ldots,\alpha+1}} \quad (62)$$

where

$$\mathcal{V}_i(m,\alpha,\beta,\eta,t) = \frac{(m+\beta+i-2)!\,(\alpha+\beta+2m+i-2)!}{(m+i-2)!\,(\beta+2m+2i-3)!\,(m+\beta-1)!} \times\frac{(\beta+m+i-2)!\,(m-1)!}{(m+\alpha+\beta-1)!\,(1+\eta)^{m+\beta}}\left(\frac{\eta t}{1+\eta}\right)^{i-1} \times{}_2F_1\left(\beta+m+i-1,\alpha+\beta+2m+i-1;\beta+2m+2i-2;\frac{\eta t}{1+\eta}\right).$$

Further manipulation of $\mathcal{V}_i(m,\alpha,\beta,\eta,t)$ in its current form is an arduous task due to the presence of the hypergeometric function. To this end, noting that $(\alpha+\beta+2m+i-1)-(\beta+2m+2i-2) = -(\alpha+1-i)$, which is a negative integer, we use the hypergeometric transformation (51) to arrive at

$$\mathcal{V}_i(m,\alpha,\beta,\eta,t) = \frac{(m+i-1)_\beta}{(m-1)_\beta}\frac{(2m+\beta+2i-2)_{\alpha-i+1}}{(m+\beta+i-1)_{\alpha-i+1}} \times\left(\frac{(\eta t)^{i-1}}{(1+\eta-\eta t)^{m+\beta+i-1}}\right) \times\sum_{\ell=0}^{\alpha-i+1}\frac{(\beta+m+i-1)_\ell(-(\alpha-i+1))_\ell}{(\beta+2m+2i-2)_\ell\ell!} \times\left(\frac{\eta t}{\eta t-1-\eta}\right)^{\ell}. \quad (63)$$

A careful inspection of (62) reveals that the suitable scaling as $m\to\infty$ would be to consider the scaled t given by $t =$

$1-\frac{x}{m^2}$. Consequently, we can write (62) as

$$\begin{aligned}&\Pr\left(x_{\max}\le 1-\frac{x}{m^2}\right)\\&=\left(1-\frac{x}{m^2}\right)^{m(\alpha+\beta+m)}\\&\times\left(\prod_{j=0}^{\alpha-1}\frac{\mathcal{S}_{k_{j+2}}\left(1-\frac{x}{m^2}\right)(\beta+2m+j-1)!}{(\beta+2m+2j)!}\right)\\&\times\det\Big[\mathcal{V}_i\left(m,\alpha,\beta,\eta,1-\frac{x}{m^2}\right)\\&\qquad\qquad\mathcal{U}_{i,j}(m,\alpha,\beta)\Big]_{\substack{i=1,\ldots,\alpha+1\\ j=2,\ldots,\alpha+1}}.\end{aligned}\tag{64}$$

Now taking the limits of the both sides of (64) as $m\to\infty$ yields

$$\begin{aligned}&\lim_{m\to\infty}\Pr(x_{\max}\le 1-\frac{x}{m^2})\\&=\exp(-x)\lim_{m\to\infty}\left(\prod_{j=0}^{\alpha-1}\frac{(\beta+2m+j-1)!}{(\beta+2m+2j)!}\mathcal{S}_{k_{j+2}}\left(1-\frac{x}{m^2}\right)\right.\\&\qquad\times\det\Big[\mathcal{V}_i\left(m,\alpha,\beta,\eta,1-\frac{x}{m^2}\right)\\&\qquad\qquad\left.\mathcal{U}_{i,j}(m,\alpha,\beta)\Big]_{\substack{i=1,2,\ldots,\alpha+1\\ j=2,3,\ldots,\alpha+1}}\right).\end{aligned}\tag{65}$$

Towards taking the limit inside the determinant, let us first consider the $\lim_{m\to\infty}\mathcal{V}_i\left(m,\alpha,\beta,\eta,1-\frac{x}{m^2}\right)$. To this end, noting that $\lim_{m\to\infty}\frac{(m+i-1)_\beta}{(m-1)_\beta}=1$ and $\lim_{m\to\infty}\frac{(2m+\beta+2i-2)_{\alpha-i+1}}{(m+\beta+i-1)_{\alpha-i+1}}=2^{\alpha-i+1}$, we may determine the limit of (63) as

$$\begin{aligned}&\lim_{m\to\infty}\mathcal{V}_i\left(m,\alpha,\beta,\eta,1-\frac{x}{m^2}\right)\\&\qquad=2^\alpha\sum_{\ell=0}^{\alpha-i+1}\left(\frac{\eta}{2}\right)^{\ell+i-1}\binom{\alpha-i+1}{\ell}=2^\alpha\mathcal{T}_i(\eta)\end{aligned}$$

where $\mathcal{T}_i(\eta)=\left(\frac{\eta}{2}\right)^{i-1}\left(1+\frac{\eta}{2}\right)^{\alpha-i+1}$.

Let us Now consider the other columns of the determinant in (65). Following (61), we may rewrite $\mathcal{U}(m,\alpha,\beta)$ as

$$\begin{aligned}\mathcal{U}_{i,j}(m,\alpha,\beta)&=(m+i-j-k_j+1)_{\alpha-i+1}\\&\qquad\times(m+\beta+j+k_j-2)_{i-1}\\&=\prod_{\ell_1=0}^{\alpha-i}(c_j-\ell_1)\prod_{\ell_2=0}^{i-2}(\Delta_m-c_j+\ell_2)\end{aligned}$$

where, $c_j=m+\alpha-j-k_j+1$ and $\Delta_m=2m+\alpha+\beta-1$. Consequently, the terms in determinant in (65) can be rearranged as shown in (66) at the bottom. Towards making the determinant independent of Δ_m, we perform the following row operations

$$R_i\to R_i+R_{i-1},\ \ i=2,3,...,\alpha+1$$

on each row, starting from the second row, to yield (67) at the bottom. To facilitate further simplification, noting that the row operation

$$\begin{aligned}R_1\to R_1+\sum_{i=2}^{\alpha+1}(-1)^{i-1}&\left(R_i\times(\Delta_m-(\alpha-1)+2(i-2))\right)\\&\times\left(2^\alpha-\sum_{j=0}^{i-2}\binom{\alpha}{j}\right),\end{aligned}$$

$$2^\alpha\begin{vmatrix}\mathcal{T}_1(\eta)&\prod_{\ell_1=0}^{\alpha-1}(c_2-\ell_1)&\cdots&\prod_{\ell_1=0}^{\alpha-1}(c_{\alpha+1}-\ell_1)\\ \mathcal{T}_2(\eta)&\prod_{\ell_1=0}^{\alpha-2}(c_2-\ell_1)(\Delta_m-c_2)&\cdots&\prod_{\ell_1=0}^{\alpha-2}(c_{\alpha+1}-\ell_1)(\Delta_m-c_{\alpha+1})\\ \vdots&\vdots&\ddots&\vdots\\ \mathcal{T}_\alpha(\eta)&c_2\prod_{\ell_2=0}^{\alpha-2}(\Delta_m-c_2+\ell_2)&\cdots&c_{\alpha+1}\prod_{\ell_2=0}^{\alpha-2}(\Delta_m-c_{\alpha+1}+\ell_2)\\ \mathcal{T}_{\alpha+1}(\eta)&\prod_{\ell_2=0}^{\alpha-1}(\Delta_m-c_2+\ell_2)&\cdots&\prod_{\ell_2=0}^{\alpha-1}(\Delta_m-c_{\alpha+1}+\ell_2)\end{vmatrix}.\tag{66}$$

$$\begin{aligned}&2^\alpha\prod_{\ell=0}^{\alpha-1}(\Delta_m-(\alpha-1)+2\ell)\begin{vmatrix}\mathcal{T}_1(\eta)&\prod_{\ell_1=0}^{\alpha-1}(c_2-\ell_1)&\cdots&\prod_{\ell_1=0}^{\alpha-1}(c_{\alpha+1}-\ell_1)\\ \frac{\mathcal{T}_2(\eta)+\mathcal{T}_1(\eta)}{\Delta_m-(\alpha-1)}&\prod_{\ell_1=0}^{\alpha-2}(c_2-\ell_1)&\cdots&\prod_{\ell_1=0}^{\alpha-2}(c_{\alpha+1}-\ell_1)\\ \vdots&\vdots&\ddots&\vdots\\ \frac{\mathcal{T}_\alpha(\eta)+\mathcal{T}_{\alpha-1}(\eta)}{\Delta_m+\alpha-3}&c_2\prod_{\ell_2=0}^{\alpha-3}(\Delta_m-c_2+\ell_2)&\cdots&c_{\alpha+1}\prod_{\ell_2=0}^{\alpha-3}(\Delta_m-c_{\alpha+1}+\ell_2)\\ \frac{\mathcal{T}_{\alpha+1}(\eta)+\mathcal{T}_\alpha(\eta)}{\Delta_m+\alpha-1}&\prod_{\ell_2=0}^{\alpha-2}(\Delta_m-c_2+\ell_2)&\cdots&\prod_{\ell_2=0}^{\alpha-2}(\Delta_m-c_{\alpha+1}+\ell_2)\end{vmatrix}\\&=\prod_{\ell=0}^{\alpha-1}(\Delta_m-(\alpha-1)+2\ell)\begin{vmatrix}2^\alpha\mathcal{T}_1(\eta)&2^\alpha\prod_{\ell_1=0}^{\alpha-1}(c_2-\ell_1)&\cdots&2^\alpha\prod_{\ell_1=0}^{\alpha-1}(c_{\alpha+1}-\ell_1)\\ \frac{\mathcal{T}_2(\eta)+\mathcal{T}_1(\eta)}{\Delta_m-(\alpha-1)}&\prod_{\ell_1=0}^{\alpha-2}(c_2-\ell_1)&\cdots&\prod_{\ell_1=0}^{\alpha-2}(c_{\alpha+1}-\ell_1)\\ \vdots&\vdots&\ddots&\vdots\\ \frac{\mathcal{T}_\alpha(\eta)+\mathcal{T}_{\alpha-1}(\eta)}{\Delta_m+\alpha-3}&c_2\prod_{\ell_2=0}^{\alpha-3}(\Delta_m-c_2+\ell_2)&\cdots&c_{\alpha+1}\prod_{\ell_2=0}^{\alpha-3}(\Delta-c_{\alpha+1}+\ell_2)\\ \frac{\mathcal{T}_{\alpha+1}(\eta)+\mathcal{T}_\alpha(\eta)}{\Delta_m+\alpha-1}&\prod_{\ell_2=0}^{\alpha-2}(\Delta_m-c_2+\ell_2)&\cdots&\prod_{\ell_2=0}^{\alpha-2}(\Delta_m-c_{\alpha+1}+\ell_2)\end{vmatrix}.\end{aligned}\tag{67}$$

set the 1^{st} element of the 1^{st} column to 1 and in view of

$$\lim_{m\to\infty}\frac{\mathcal{T}_i(\eta)+\mathcal{T}_{i-1}(\eta)}{\Delta_m-(\alpha-1)+2(i-2)}=0,\ \ i=2,3,\ldots,\alpha+1,$$

we again apply the row operation $R_i \to R_i + R_{i-1}$, for $i = 3, 4, ..., \alpha+1$, repeatedly to obtain

$$\prod_{j=0}^{\alpha-1}\prod_{\ell_j=0}^{j}(\Delta_m-j+2\ell_j)\times\begin{vmatrix}1 & *_2 & \cdots & *_{\alpha+1}\\ 0 & \prod_{\ell_1=0}^{\alpha-2}(c_2-\ell_1) & \cdots & \prod_{\ell_1=0}^{\alpha-2}(c_{\alpha+1}-\ell_1)\\ \vdots & \vdots & \ddots & \vdots\\ 0 & c_2 & \cdots & c_{\alpha+1}\\ 0 & 1 & \cdots & 1\end{vmatrix}.$$

Here the exact form of the $*$ marked entries are tacitly avoided, since they do not contribute to the determinant evaluation. As such, by expanding the determinant using the first column, we obtain (68) as shown below. The below determinant can be simplified using [59, Lemma A.1] to yield

$$\prod_{j=0}^{\alpha-1}\prod_{\ell_j=0}^{j}(\Delta_m-j+2\ell_j)\Delta_\alpha(\tilde{\mathbf{c}})$$

where $\Delta_\alpha(\tilde{\mathbf{c}}) = \prod_{1\le j<i\le\alpha}(\tilde{c}_i(k_{i+1})-\tilde{c}_j(k_{j+1}))$ with $\tilde{\mathbf{c}} = \{\tilde{c}_1(k_2), \tilde{c}_2(k_3), \cdots, \tilde{c}_\alpha(k_{\alpha+1})\}$ and $\tilde{c}_j(k_{j+1}) = j + k_{j+1}$. Now we substitute the above result into (65) to obtain

$$\begin{aligned}
&\lim_{m\to\infty}\Pr\left(x_{\max}\le 1-\frac{x}{m^2}\right)\\
&=\exp(-x)\lim_{m\to\infty}\left(\prod_{j=0}^{\alpha-1}\mathcal{S}_{k_{j+2}}\left(1-\frac{x}{m^2}\right)\right.\\
&\qquad\times\left(\prod_{j=0}^{\alpha-1}\frac{(\beta+2m+j-1)!}{(\beta+2m+2j)!}\right)\\
&\qquad\left.\times\prod_{j=0}^{\alpha-1}\prod_{\ell_j=0}^{j}(\Delta_m-j+2\ell_j)\Delta_\alpha(\tilde{\mathbf{c}})\right)\\
&=\exp(-x)\lim_{m\to\infty}\left(\prod_{j=0}^{\alpha-1}\mathcal{S}_{k_{j+2}}\left(1-\frac{x}{m^2}\right)\right.\\
&\qquad\left.\times\prod_{j=0}^{\alpha-1}\prod_{\ell_j=0}^{j}\frac{(2m+\beta+\alpha-j+2l-1)}{2m+\beta+2j-l}\Delta_\alpha(\tilde{\mathbf{c}})\right)\\
&=\exp(-x)\lim_{m\to\infty}\left(\prod_{j=0}^{\alpha-1}\mathcal{S}_{k_{j+2}}\left(1-\frac{x}{m^2}\right)\Delta_\alpha(\tilde{\mathbf{c}})\right).
\end{aligned}$$

For notational convenience, the index j is shifted forward by one unit to yield

$$\begin{aligned}
&\lim_{m\to\infty}\Pr\left(x_{\max}\le 1-\frac{x}{m^2}\right)\\
&\qquad=\exp(-x)\lim_{m\to\infty}\left(\prod_{j=1}^{\alpha}\mathcal{S}_{k_j}\left(1-\frac{x}{m^2}\right)\Delta_\alpha(\mathbf{c})\right)
\end{aligned}\tag{69}$$

where $\mathbf{c} = \{c_1(k_1), c_2(k_1), \cdots, c_\alpha(k_\alpha)\}$ with $c_j(k_j) = j + k_j$. Having noted that $\Delta_\alpha(\mathbf{c})$ is independent of m and

$$\lim_{m\to\infty}\frac{(m+\alpha-j-k_j+1)_{k_j}}{m^{k_j}}=1,$$
$$\lim_{m\to\infty}\frac{(m+\beta+j-1)_{k_j}}{m^{k_j}}=1,$$

we evaluate the limit of $\mathcal{S}_{k_j}\left(1-\frac{x}{m^2}\right)$ as

$$\begin{aligned}
&\lim_{m\to\infty}\mathcal{S}_{k_j}\left(1-\frac{x}{m^2}\right)\\
&=\lim_{m\to\infty}\sum_{k_j=0}^{m+\alpha-j}(-1)^{k_j}\frac{(-(m+\alpha-j))_{k_j}(m+\beta+j-1)_{k_j}}{k_j!\,(j+k_j-1)!\,m^{2k_j}}\\
&\qquad\times\frac{x^{k_j}}{\left(1-\frac{x}{m^2}\right)^{k_j}}\\
&=\lim_{m\to\infty}\sum_{k_j=0}^{m+\alpha-j}\frac{(m+\alpha-j-k_j+1)_{k_j}}{m^{k_j}}\frac{(m+\beta+j-1)_{k_j}}{m^{k_j}}\\
&\qquad\times\frac{x^{k_j}}{k_j!\,(k_j+j-1)!}\frac{1}{\left(1-\frac{x}{m^2}\right)^{k_j}}\\
&=\sum_{k_j=0}^{\infty}\frac{x^{k_j}}{k_j!\,(k_j+j-1)!}.
\end{aligned}$$

Therefore, (69) simplifies to

$$\begin{aligned}
&\lim_{m\to\infty}\Pr\left(x_{\max}\le 1-\frac{x}{m^2}\right)\\
&\quad=\exp(-x)\sum_{k_1=0}^{\infty}\sum_{k_2=0}^{\infty}\cdots\sum_{k_\alpha=0}^{\infty}\prod_{j=1}^{\alpha}\frac{x^{k_j}}{k_j!\,(k_j+j-1)!}\Delta_\alpha(\mathbf{c}),
\end{aligned}$$

from which we obtain using [60, Appendix B]

$$\begin{aligned}
&\lim_{m\to\infty}\Pr\left(x_{\max}\le 1-\frac{x}{m^2}\right)\\
&\qquad=\exp(-x)\det\left[\mathcal{I}_{j-i}(2\sqrt{x})\right]_{i,j=1,2,\cdots,\alpha}.
\end{aligned}$$

The above result implies that,

$$\begin{aligned}
&\lim_{m\to\infty}\Pr(m^2(1-x_{\max})\le x)\\
&\qquad=1-\exp(-x)\det\left[\mathcal{I}_{j-i}(2\sqrt{x})\right]_{i,j=1,2,\cdots,\alpha}.
\end{aligned}$$

$$\prod_{j=0}^{\alpha-1}\prod_{\ell_j=0}^{j}(\Delta_m-j+2\ell_j)\begin{vmatrix}\prod_{\ell_1=0}^{\alpha-2}(c_2-\ell_1) & \prod_{\ell_1=0}^{\alpha-2}(c_3-\ell_1) & \cdots & \prod_{\ell_1=0}^{\alpha-2}(c_{\alpha+1}-\ell_1)\\ \prod_{\ell_1=0}^{\alpha-3}(c_2-\ell_1) & \prod_{\ell_1=0}^{\alpha-3}(c_3-\ell_1) & \cdots & \prod_{\ell_1=0}^{\alpha-3}(c_{\alpha+1}-\ell_1)\\ \vdots & \vdots & \ddots & \vdots\\ c_2 & c_3 & \cdots & c_{\alpha+1}\\ 1 & 1 & \cdots & 1\end{vmatrix}.\tag{68}$$

Finally, noting that

$$\begin{aligned}\lim_{m\to\infty} F^{(\alpha)}_{m^2(1-x_{\max})}(x) &= \lim_{m\to\infty} \Pr\left(m^2(1-x_{\max}) \le x\right)\\ &= \lim_{m\to\infty} F^{(\alpha)}_{\frac{m^2}{1+\lambda_{\max}}}(x)\\ &= F^{(\alpha)}_{1/X}(x),\end{aligned}$$

we may use the continuous mapping theorem [61] to obtain (22), which concludes the proof.

REFERENCES

[1] L. D. Chamain, P. Dharmawansa, S. Atapattu, and C. Tellambura, "Detection of a signal in colored noise: A random matrix theory based analysis," in *Proc. IEEE Global Telecommn. Conf. (GLOBECOM)*, Hawaii, USA, Dec. 2019.

[2] H. L. V. Trees, *Detection, Estimation, and Modulation Theory*. New York Chichester: Wiley, 2001.

[3] ——, *Optimum Array Processing*. New York: Wiley-Interscience, 2002.

[4] R. R. Nadakuditi and A. Edelman, "Sample eigenvalue based detection of high-dimensional signals in white noise using relatively few samples," *IEEE Trans. Signal Process.*, vol. 56, no. 7, pp. 2625–2638, Jul. 2008.

[5] R. R. Nadakuditi and J. W. Silverstein, "Fundamental limit of sample generalized eigenvalue based detection of signals in noise using relatively few signal-bearing and noise-only samples," *IEEE J. Sel. Topics Signal Process.*, vol. 4, no. 3, pp. 468–480, Jun. 2010.

[6] P. Bianchi, M. Debbah, M. Maida, and J. Najim, "Performance of statistical tests for single-source detection using random matrix theory," *IEEE Trans. Inf. Theory*, vol. 57, no. 4, pp. 2400–2419, Apr. 2011.

[7] R. Couillet and W. Hachem, "Fluctuations of spiked random matrix models and failure diagnosis in sensor networks," *IEEE Trans. Inf. Theory*, vol. 59, no. 1, pp. 509–525, Jan. 2013.

[8] N. Asendorf and R. R. Nadakuditi, "The performance of a matched subspace detector that uses subspaces estimated from finite, noisy, training data," *IEEE Trans. Signal Process.*, vol. 61, no. 8, pp. 1972–1985, Apr. 2013.

[9] ——, "Improved detection of correlated signals in low-rank-plus-noise type data sets using informative canonical correlation analysis (ICCA)," *IEEE Trans. Inf. Theory*, vol. 63, no. 6, pp. 3451–3467, Jun. 2017.

[10] R. Couillet and M. Debbah, *Random Matrix Methods for Wireless Communications*. Cambridge University Press, New York, 2011.

[11] P. Bianchi, M. Debbah, M. Maida, and J. Najim, "Performance of statistical tests for single-source detection using random matrix theory," *IEEE Trans. Inf. Theory*, vol. 57, no. 4, pp. 2400–2419, Apr. 2011.

[12] K. V. Mardia, J. T. Kent, and J. M. Bibby, *Multivariate Analysis*. Academic Press, London, 1979.

[13] J. Baik, G. B. Arous, and S. Péché, "Phase transition of the largest eigenvalue for non-null complex sample covariance matrices," *Ann. Probab.*, vol. 33, no. 5, pp. 1643–1697, 2005.

[14] J. Baik and J. W. Silverstein, "Eigenvalues of large sample covariance matrices of spiked population models," *J. Multivariate Anal.*, vol. 97, no. 6, pp. 1382–1408, 2006.

[15] D. Paul, "Asymptotics of sample eigenstructure for a large dimensional spiked covariance model," *Statist. Sinica*, vol. 17, no. 4, pp. 1617–1642, 2007.

[16] N. E. Karoui, "Tracy-Widom limit for the largest eigenvalue of a large class of complex sample covariance matrices," *Ann. Probab.*, vol. 35, no. 2, pp. 663–714, 2007.

[17] D. C. Hoyle and M. Rattray, "Statistical mechanics of learning multiple orthogonal signals: Asymptotic theory and fluctuation effects," *Phys. Rev. E (3)*, vol. 75, no. 1, p. 016 101, 2007.

[18] B. Nadler, "Finite sample approximation results for principal component analysis: A matrix perturbation approach," *Ann. Statist.*, vol. 36, no. 6, pp. 2791–2817, 2008.

[19] E. Maris, "A resampling method for estimating the signal subspace of spatio-temporal EEG/MEG data," *IEEE Trans. Biomed. Eng.*, vol. 50, no. 8, pp. 935–949, Aug 2003.

[20] K. Sekihara, D. Poeppel, A. Marantz, H. Koizumi, and Y. Miyashita, "Noise covariance incorporated MEG-MUSIC algorithm: a method for multiple-dipole estimation tolerant of the influence of background brain activity," *IEEE Trans. Biomed. Eng.*, vol. 44, no. 9, pp. 839–847, Sep. 1997.

[21] ——, "MEG spatio-temporal analysis using a covariance matrix calculated from nonaveraged multiple-epoch data," *IEEE Trans. Biomed. Eng.*, vol. 46, no. 5, pp. 515–521, May 1999.

[22] J. Vinogradova, R. Couillet, and W. Hachem, "Statistical inference in large antenna arrays under unknown noise pattern," *IEEE Trans. Signal Process.*, vol. 61, no. 22, pp. 5633–5645, Nov. 2013.

[23] S. Hiltunen, P. Loubaton, and P. Chevalier, "Large system analysis of a GLRT for detection with large sensor arrays in temporally white noise," *IEEE Trans. Signal Process.*, vol. 63, no. 20, pp. 5409–5423, Oct. 2015.

[24] I. M. Johnstone and B. Nadler, "Roy's largest root test under rank-one alternatives," *Biometrika*, vol. 104, no. 1, pp. 181–193, 2017.

[25] P. Dharmawansa, B. Nadler, and O. Shwartz, "Roy's largest root under rank-one perturbations: The complex valued case and applications," *J. Multivar. Anal.*, vol. 174, p. 104524, Nov. 2019.

[26] P. Dharmawansa, I. M. Johnstone, and A. Onatski, "Local asymptotic normality of the spectrum of high-dimensional spiked F-ratios," *arXiv:1411.3875 [math.ST]*, Nov. 2014.

[27] Q. Wang and J. Yao, "Extreme eigenvalues of large-dimensional spiked Fisher matrices with application," *Ann. Statist.*, vol. 45, no. 1, pp. 415–460, Feb. 2017.

[28] A. Dubbs and A. Edelman, "The Beta-MANOVA ensemble with general covariance," *Random Matrices: Theory and Applications*, vol. 03, no. 01, p. 1450002, Jan. 2014.

[29] R. Kan and P. Koev, "Densities of the extreme eigenvalues of Beta–MANOVA matrices," *Random Matrices: Theory and Applications*, vol. 08, no. 01, p. 1950002, Jan. 2019.

[30] P. Koev and I. Dumitriu, "Distribution of the extreme eigenvalues of the complex Jacobi random matrix ensemble," *SIAM. J. Matrix Anal. & Appl.*, 2005.

[31] I. Dumitriu, "Smallest eigenvalue distributions for two classes of β - Jacobi ensembles," *J. Math. Phys.*, vol. 53, no. 10, p. 103301, Oct. 2012.

[32] I. Dumitriu and P. Koev, "Distributions of the extreme eigenvalues of Beta-Jacobi random matrices," *SIAM J. Matrix Anal. & Appl.*, vol. 30, no. 1, pp. 1–6, Jan. 2008.

[33] L. Moreno-Pozas, D. Morales-Jimenez, and M. R. McKay, "Extreme eigenvalue distributions of Jacobi ensembles: New exact representations, asymptotics and finite size corrections," *Nuclear Physics B*, vol. 947, p. 114724, Oct. 2019.

[34] P. Dharmawansa and I. M. Johnstone, "Joint density of eigenvalues in spiked multivariate models," *Stat*, vol. 31, pp. 240–249, Jul. 2014.

[35] A. Onatski, "Detection of weak signals in high-dimensional complex-valued data," *Random Matrices: Theory and Applications*, vol. 03, no. 01, p. 1450001, 2014.

[36] D. Passemier, M. R. McKay, and Y. Chen, "Hypergeometric functions of matrix arguments and linear statistics of multi-spiked Hermitian matrix models," *J. Multivar. Anal.*, vol. 139, pp. 124–146, 2015.

[37] M. Y. Mo, "The rank 1 real Wishart spiked model," *Commun. Pure Appl. Math.*, no. 65, pp. 1528–1638, Nov. 2012.

[38] D. Wang, "The largest eigenvalue of real symmetric, Hermitian and Hermitian self-dual random matrix models with rank one external source, part I," *J. Stat. Phys.*, vol. 146, no. 4, pp. 719–761, 2012.

[39] I. M. Johnstone and A. Onatski, "Testing in high-dimensional spiked models," *arXiv:1509.07269 [math.ST]*, Feb. 2018.

[40] Z. Bao, G. Pan, and W. Zhou, "Universality for the largest eigenvalue of sample covariance matrices with general population," *Ann. Statist.*, vol. 43, no. 1, pp. 382–421, Feb. 2015.

[41] R. L. Dykstra and J. E. Hewett, "Positive dependence of the roots of a Wishart matrix," *Ann. Stat.*, vol. 6, no. 1, pp. 235–238, 1978.

[42] R. J. Muirhead, *Aspects of Multivariate Statistical Theory*. John Wiley & Sons, 2009, vol. 197.

[43] M. L. Mehta, *Random Matrices*. Academic Press, 2004, vol. 142.

[44] P. J. Forrester, *Log-Gases and Random Matrices (LMS-34)*. Princeton University Press, 2010.

[45] A. T. James, "Distributions of matrix variates and latent roots derived from normal samples," *The Annals of Mathematical Statistics*, pp. 475–501, 1964.

[46] I. M. Johnstone, "Multivariate analysis and Jacobi ensembles: Largest eigenvalue, Tracy-Widom limits and rates of convergence," *Ann. Stat.*, vol. 36, no. 6, pp. 2638–2716, 2008.

[47] T. Jiang, "Limit theorems for Beta-Jacobi ensembles," *Bernoulli*, vol. 19, no. 3, pp. 1028–1046, 08 2013.

[48] H. M. Ramli, E. Katzav, and I. P. Castillo, "Spectral properties of the Jacobi ensembles via the Coulomb gas approach," *J. Phys. A: Mathematical and Theoretical*, vol. 45, no. 46, p. 465005, Nov. 2012.

[49] D. Holcomb and G. R. Moreno Flores, "Edge scaling of the β-Jacobi ensemble," *J. Stat. Phys*, vol. 149, no. 6, pp. 1136–1160, Dec. 2012.

[50] D.-Z. Liu, "Limits for circular Jacobi beta-ensembles," *J. Approx. Theory*, vol. 215, pp. 40–67, Mar. 2017.

[51] P. J. Forrester, "Probability densities and distributions for spiked and general variance Wishart β-ensembles," *Random Matrices: Theory and Applications*, vol. 2, no. 4, 2013.
[52] L. C. Andrews, *Special Functions of Mathematics for Engineers*. SPIE Press, 1998.
[53] C. G. Khatri, "On the moments of traces of two matrices in three situations for complex multivariate normal populations," *Sankhyā*, vol. 32, pp. 65–80, 1970.
[54] K. W. Wachter, "The strong limits of random matrix spectra for sample matrices of independent elements," *Ann. Probab.*, vol. 6, no. 1, pp. 1–18, Feb. 1978.
[55] J. Silverstein, "The limiting eigenvalue distribution of a multivariate F matrix," *SIAM J. Math. Anal.*, vol. 16, no. 3, pp. 641–646, 1985.
[56] F. Topsøe, "Some bounds for the logarithmic function," *RGMIA Res. Rep. Collection*, vol. 7, no. 2, 2004, Art. ID. 6.
[57] A. Erdélyi, *Tables of Integral Transforms, Vol. 1 and Vol. 2*. McGraw-Hill, New York, 1954.
[58] M. Abramowitz and I. A. Stegun, *Handbook of mathematical functions: with formulas, graphs, and mathematical tables*. Courier Corporation, 1964, vol. 55.
[59] P. Dharmawansa, M. R. McKay, and Y. Chen, "Distributions of Demmel and related condition numbers," *SIAM. J. Matrix Anal. & Appl.*, vol. 34, no. 1, pp. 257–279, 2013.
[60] P. Dharmawansa, "Some new results on the eigenvalues of complex non-central Wishart matrices with a rank-1 mean," *J. Multivar. Anal.*, vol. 149, pp. 30–53, 2016.
[61] A. W. van der Vaart, *Asymptotic Statistics*. Cambridge University Press, 1998.

Lahiru D. Chamain is currently a PhD candidate in Electrical and Computer Engineering (ECE) at University of California Davis, USA. He received his M.Sc. degree in ECE from UC Davis in 2020 majoring in Signal Processing for Image Analysis and minoring in Machine Learning and B.Sc. degree from University of Moratuwa, Sri Lanka in 2016 majoring in Electronics and Telecommunication Engineering. His research interests align with image/video compression for deep learning, internet of things, and detection and estimation theory.

Prathapasinghe Dharmawansa (M'09) received the B.Sc. and M.Sc. degrees in Electronic and Telecommunication Engineering from the University of Moratuwa, Moratuwa, Sri Lanka in 2003 and 2004 respectively, and the Doctor of Engineering (D. Eng.) degree in Information and Communications Technology from the Asian Institute of Technology, Thailand in 2007. Subsequently he joined the Department of Electronic and Computer Engineering, Hong Kong University of Science and Technology (HKUST) as a Research Associate. From October 2011 to September 2012, he was with the Department of Communication and Networking, Aalto School of Electrical Engineering, Aalto University (formerly Helsinki University of Technology (HUT)), Finland as a Postdoctoral Researcher. From October 2012 to August 2015, he was with the Department of Statistics, Stanford University, CA. He currently is a Senior Lecturer in the Department of Electronic and Telecommunication Engineering, University of Moratuwa, Sri Lanka. His research interests are in wireless communications, signal processing, random matrix theory, and high dimensional statistics. Dr. Dharmawansa received a Best Paper Award in Communication Theory at IEEE ICC 2011.

Saman Atapattu (SM'19) received the B.Sc. degree in Electrical and Electronics Engineering from the University of Peradeniya, Sri Lanka, the M.Eng. degree in Telecommunications from Asian Institute of Technology (AIT), Thailand, and the Ph.D. degree in Electrical Engineering from the University of Alberta, Canada. He is currently working with the Department of Electrical and Electronic Engineering, the University of Melbourne, Australia. His research interests include wireless communications and signal processing.

Chintha Tellambura (F'11) received the B.Sc. degree (with first-class honor) from the University of Moratuwa, Sri Lanka, the MSc degree in Electronics from King's College, University of London, United Kingdom, and the PhD degree in Electrical Engineering from the University of Victoria, Canada.

He was with Monash University, Australia, from 1997 to 2002. Presently, he is a Professor with the Department of Electrical and Computer Engineering, University of Alberta. His current research interests include the design, modelling and analysis of cognitive radio, heterogeneous cellular networks, 5G wireless networks and machine learning algorithms.

Prof. Tellambura served as an editor for both IEEE Transactions on Communications (1999-2011) and IEEE Transactions on Wireless Communications (2001-2007) and for the latter he was the Area Editor for Wireless Communications Systems and Theory during 2007-2012. He has received best paper awards in the Communication Theory Symposium in 2012 IEEE International Conference on Communications (ICC) in Canada and 2017 ICC in France. He is the winner of the prestigious McCalla Professorship and the Killam Annual Professorship from the University of Alberta. In 2011, he was elected as an IEEE Fellow for his contributions to physical layer wireless communication theory. In 2017, he was elected as a Fellow of Canadian Academy of Engineering. He has authored or coauthored over 500 journal and conference papers with an H-index of 75 (Google Scholar).